Promjena ekspresije gena REL, PDL1 i CXCL10 faktorom nekroze tumora alfa i interferonom gama u stanicama karcinoma vrata maternice i primarnog medijastinalnog B-staničnog limfoma čovjeka

Mihalić, Valentino

University of Zagreb
Faculty of Science
Department of Biology

Valentino Mihalić

Tumor Necrosis Factor-α and Interferon-γ induced changes of *REL*, *PDL1*, and *CXCL10* expression in human cervical carcinoma and primary mediastinal B-cell lymphoma cell lines

Master thesis

Zagreb, 2024.

Sveučilište u Zagrebu
Prirodoslovno-matematički fakultet
Biološki odsjek

Valentino Mihalić

Promjena ekspresije gena *REL*, *PDL1* i *CXCL10* faktorom nekroze tumora α i interferonom γ u stanicama karcinoma vrata maternice i primarnog medijastinalnog B-staničnog limfoma čovjeka

Diplomski rad

Zagreb, 2024.

Ovaj rad je izrađen na Zavodu za molekularnu biologiju Prirodoslovno-matematičkog fakulteta u Zagrebu, pod mentorstvom prof. dr. sc. Petre Korać, te komentorstvom dr. sc. Paule Gršković. Rad je predan na ocjenu Biološkom odsjeku Prirodoslovno-matematičkog fakulteta Sveučilišta u Zagrebu radi stjecanja zvanja magistar molekularne biologije (mag. biol. mol.).

Acknowledgements

This research would not have been possible without the support of Dr. K. Mellert, Dr. S. Bruderlein and Prof. Dr. P. Möller, whom I am very grateful for providing the cell line MedB-1. I would also like to thank my mentor, prof. Petra Korać, PhD, and my co-mentor Paula Gršković, PhD, for all the help along the way. Finally, a big thank you to my friends and family, whose valuable support and guidance made this report possible.

TEMELJNA DOKUMENTACIJSKA KARTICA

Sveučilište u Zagrebu
Prirodoslovno-matematički fakultet
Biološki odsjek Diplomski rad

Promjena ekspresije gena *REL*, *PDL1* i *CXCL10* faktorom nekroze tumora α i interferonom γ u stanicama karcinoma vrata maternice i primarnog medijastinalnog B-staničnog limfoma čovjeka

Valentino Mihalić

Rooseveltov trg 6, 10000 Zagreb, Hrvatska

Primarni medijastinalni B-stanični limfom (PMBCL, od eng. *primary mediastinal B-cell lymphoma*), limfom koji dijeli neke značajke s difuznim velikim B-staničnim limfomom (DLBCL, od eng. *diffuse large B-cell lymphoma*) i klasičnim Hodgkinovim limfomom (cHL, od eng. *classical Hodgkin lymphoma*), obilježen je konstitutivnom aktivnošću signalnih putova NF-κB i JAK-STAT, koji dovode do transkripcije gena uključenih u imunosnu modulaciju i preživljavanje stanica. Cilj ovog istraživanja bio je analizirati obrasce ekspresije specifičnih gena u staničnim linijama PMBCL-a MedB-1 i Karpas 1106p te u staničnoj liniji HeLa, koja potječe iz ljudskog karcinoma vrata maternice, nakon tretmana različitim dozama proupalnih citokina TNF-α i IFN-γ. Osnovne razine ekspresije gena *REL*, *CXCL10* i *PDL1* bile su više u staničnim linijama modelima PMBCL-a nego u stanicama HeLa. 48 sati nakon tretmana citokinom TNF-α, stanice MedB-1 pokazale su značajno povećanje ekspresije gena *REL* i *PDL1* pri dozama od 10, 20 i 50 ng/ml. Stanice HeLa pokazale su značajno povećanje ekspresije gena *CXCL10* 24 sata nakon tretmana s 5, 10 i 20 ng/ml TNF-α, za razliku od stanica MedB-1 i Karpas 1106p, koje nisu pokazale promjene u ekspresiji gena *CXCL10*. Nakon tretmana IFN-γ, sve stanične linije pokazale su značajno povećanje ekspresije gena *CXCL10* i *PDL1*, pri čemu su stanice HeLa pokazale najveći porast ekspresije gena *PDL1*.

Ključne riječi: MedB-1, Karpas 1106p, HeLa, NF-κB, JAK-STAT
(41 stranica, 10 slika, 9 tablica, 77 literaturnih navoda, jezik izvornika: engleski)
Rad je pohranjen u Središnjoj biološkoj knjižnici

Mentor: prof. dr. sc. Petra Korać
Komentor: dr. sc. Paula Gršković

Ocjenitelji:
prof. dr. sc. Petra Korać

prof. dr. sc. Inga Urlić
izv. prof. dr. sc. Tomislav Ivanković
Rad prihvaćen: 05.09.2024.

BASIC DOCUMENTATION CARD

University of Zagreb
Faculty of Science
Department of Biology

Master thesis

Tumor Necrosis Factor-α and Interferon-γ induced changes of *REL*, *PDL1*, and *CXCL10* expression in human cervical carcinoma and primary mediastinal B-cell lymphoma cell lines

Valentino Mihalić

Rooseveltov trg 6, 10000 Zagreb, Croatia

Primary mediastinal B-cell lymphoma (PMBCL), a type of lymphoma that shares some features with diffuse large B-cell lymphoma (DLBCL) and classical Hodgkin lymphoma (cHL), is marked by constitutive activity of the NF-κB and JAK-STAT signaling pathways, which lead to the transcription of genes involved in immune modulation and cell survival. The aim of this research was to analyze the expression patterns of specific genes in the PMBCL cell lines MedB-1 and Karpas 1106p and in the HeLa cell line, which originates from human cervical cancer, after treatment with different doses of the pro-inflammatory cytokines TNF-α and IFN-γ. Baseline gene expression levels of *REL*, *CXCL10*, and *PDL1* were higher in PMBCL-derived cell lines than in HeLa cells. 48 hours after TNF-α treatment, MedB-1 cells showed a significant increase in *REL* and *PDL1* gene expression at doses of 10, 20 and 50 ng/ml. HeLa cells showed a significant increase in *CXCL10* gene expression 24 hours after treatment with 5, 10 and 20 ng/ml TNF-α, in contrast to MedB-1 and Karpas 1106p cells, which did not show changes in *CXCL10* gene expression. After IFN-γ treatment, all cell lines showed a significant increase in *CXCL10* and *PDL1* gene expression, with HeLa cells showing the highest increase in *PDL1* gene expression.

Keywords: MedB-1, Karpas 1106p, HeLa, NF-κB, JAK-STAT
(41 pages, 10 figures, 9 tables, 77 references, original in: English)
Thesis is deposited in Central Biological Library.

Mentor: Petra Korać, PhD
Co-mentor: Paula Gršković, PhD

Reviewers:
Prof. Petra Korać, PhD
Prof. Inga Urlić, PhD
Assoc. Prof. Tomislav Ivanković, PhD
Thesis accepted: September 5th, 2024

Contents

Abbreviations

APCs – antigen-presenting cells

cHL – classical Hodgkin lymphoma

c-REL – reticuloendotheliosis viral oncogene homolog

DLBCL – diffuse large B-cell lymphoma

HPV – human papillomavirus

IFN-γ – interferon-gamma

JAK – Janus kinase

MHC – major histocompatibility complex

NF-κB – nuclear factor-kappa B

NHL – non-Hodgkin lymphoma

NK – natural killer

PD-L1 – programmed death ligand-1

PD-1 – programmed death-1

PMBCL – primary mediastinal B-cell lymphoma

STAT – signal transducer and activator of transcription

SOCS – suppressors of cytokine signaling

TME – tumor microenvironment

TNF-α – tumor necrosis factor-alpha

TNFs – tumor necrosis factors

1. Introduction

1.1. Cytokines and their role in cancer and immunity

Cytokines are small proteins that modulate and regulate immunological responses, inflammation, and hematopoiesis (Dinarello, 2007). They are produced by various types of cells, including immune cells like macrophages, B and T lymphocytes, and mast cells, as well as non-immune cells like endothelial cells and fibroblasts. By binding to specific receptors on target cells, cytokines activate signaling pathways that can lead to cell proliferation, differentiation, and apoptosis (O'Shea et al., 2002). Because of their great diversity, they are divided into several classes based on their structure and function. These classes include interleukins, interferons, tumor necrosis factors (TNFs), chemokines, and colony-stimulating factors (Akdis et al., 2011). Interleukins are mainly produced by leukocytes and facilitate their communication between each other, while interferons are known for their role in defense against viruses. TNFs are involved in systemic inflammation and can induce apoptotic cell death, chemokines guide cell migration during immune responses, and colony-stimulating factors stimulate blood cell production from hematopoietic stem cells.

In the context of cancer, cytokines have a dual role; they can either promote tumor progression or contribute to anti-tumor immunity depending on the context and balance of different cytokines in the tumor microenvironment (TME). TME is a complex system made from tumor cells, stromal cells, and infiltrating immune cells, all of which communicate through cytokine signaling. Pro-inflammatory cytokines like tumor necrosis factor-alpha (TNF-α) and interferon-gamma (IFN-γ) can trigger immune responses that attack tumor cells (Dranoff, 2004; Lienard et al., 1992). On the other hand, some cytokines can foster an immunosuppressive environment that supports tumor growth and protects the tumor from immune system attacks.

Interleukins and chemokines are also crucial in malignant diseases. IL-6, for instance, is associated with chronic inflammation and has been linked to cancer progression by enhancing the survival and proliferation of malignant cells (Kishimoto, 2005). On the other hand, IL-10 is an anti-inflammatory cytokine that can suppress anti-tumor immunity, aiding malignant cells in evading the immune system (Moore et al., 2001). Chemokines, which direct the migration of immune cells, can either promote anti-tumor responses or help recruit immunosuppressive cells, depending on the context and the specific cells they attract. For example, chemokine CXCL10, also known as interferon gamma-induced protein 10 (IP-10), attracts T cells, natural killer (NK) cells, and monocytes to sites of inflammation. It is produced by various cells, including

monocytes, endothelial cells, and fibroblasts, in response to interferon-gamma (IFN-γ). Elevated levels of CXCL10 have been associated with various inflammatory diseases, but have also shown anti-tumor properties (Karin & Razon, 2018; Arenberg et al., 2001). Among the various cytokines, TNF-α and IFN-γ are particularly important due to their complex and sometimes contradictory roles in tumor progression and immunity.

1.2. Tumor necrosis factor-alpha

TNF-α is an inflammatory cytokine mainly secreted by macrophages in response to infection and inflammation. It was named based on its capacity to cause necrotic tumor cell death *in vitro* (Sharif et al., 2020). In addition to macrophages, other immune cells including T and B lymphocytes, NK cells, and dendritic cells have the ability to secrete TNF-α. It affects many different types of cells, such as fibroblasts, endothelial cells, and multiple tumor cell types.

TNF-α is involved in the acute phase of inflammation, capable of inducing fever, apoptotic cell death, sepsis, and cachexia (Bradley, 2008). It plays a significant role in various inflammatory and autoimmune diseases such as rheumatoid arthritis, inflammatory bowel disease, and psoriasis (Tracey et al., 2008). In the context of malignant diseases, it has the ability to impede the growth of tumors by either inducing direct cell death in tumor cells or by triggering immunological responses that are detrimental to tumor development. In contrast, continuous production of TNF-α can stimulate the growth of tumors by promoting processes such as the formation of new blood vessels (angiogenesis), the multiplication of tumor cells, and the spread of tumor to other parts of the body (metastasis). The contrasting nature of TNF-α in cancer requires nuanced approach to therapy, as its inhibition can be beneficial in certain scenarios but detrimental in others (Balkwill, 2009; Sharif et al., 2020).

TNF-α exerts its biological effects through two unique cell surface receptors, TNFR1 and TNFR2, which are present on nearly all cell types and elicit varied signaling and functional results. TNFR1 is involved in TNF-α's pro-inflammatory effects, while TNFR2 is involved in tissue regeneration and immune regulation (Sharif et al., 2020).

Binding of TNF-α to its receptors triggers a series of intracellular signaling events that activate two important pathways in human B cells, NF-κB and JAK-STAT (Miscia et al., 2002). These pathways play a critical role in regulating the cellular response to inflammatory and immunological stressors.

The NF-κB pathway is central to the regulation of genes involved in immune response, inflammation, and cell survival. The activation of NF-κB by TNF-α occurs when TNF receptors

are engaged, resulting in the recruitment of adaptor proteins such TRADD and RIPK1. These adaptor proteins then assist the activation of the IKK complex. IKK complex phosphorylates the inhibitor IκB, marking it for ubiquitination and eventual proteasomal destruction. When IκB degrades, it releases the NF-κB dimers. These dimers then move to the nucleus and start the process of transcribing several genes that are important for immunological function, inflammatory responses, and apoptosis prevention. The regulation of this pathway is complex, involving multiple levels of control, including the sequestration of NF-κB in the cytoplasm by IκB under normal conditions and its release and relocation into the nucleus upon activation (Vallabhapurapu & Karin, 2009).

The Janus kinase-signal transducer and activator of transcription (JAK-STAT) pathway is another signaling cascade that is initiated by TNF-α in healthy and malignant B cells (Miscia et al., 2002). It transmits information from cytokines outside the cell to the nucleus. This system influences gene expression, which controls cell development, differentiation, and immune function. Cytokines bind to their receptors, leading to the activation of JAK kinases, which subsequently phosphorylate STAT proteins. The phosphorylated STATs form dimers and go to the nucleus, where they attach to DNA in order to control gene transcription. The specificity of the JAK-STAT signaling cascade is regulated by the distinct combinations of JAK and STAT proteins that are activated, which is controlled by the precise interactions between cytokines and receptors (Levy & Darnell, 2002; Aaronson & Horvath, 2002; Shuai & Liu, 2003). However, that the JAK-STAT pathway is primarily activated by IFN-γ.

1.3. Interferon-gamma

IFN-γ is produced by cells of the immune system, such as NK cells, natural killer T cells, and T helper cells, particularly the T helper 1 (Th1) subtype. Additionally, it can be produced by cytotoxic T cells and specific antigen-presenting cells (APCs) such as macrophages and dendritic cells. IFN-γ is usually produced as a reaction to infection or immunological challenges (Schroder et al., 2004).

IFN-γ attaches to its distinct receptors on the surface of cells, known as IFN-γ receptors 1 and 2 (IFNGR1 and IFNGR2), resulting in the recruitment and stimulation of JAK1 and JAK2 kinases (Bach et al., 1997; Schroder et al., 2004). These enzymes provide phosphate groups to important tyrosine residues on the receptor, which then serve as binding sites for STAT1 proteins. After being recruited to the receptor, STAT1 proteins undergo phosphorylation, which causes them to form dimers and then go into the nucleus. Once in the nucleus, they attach to

gamma-activated sequences (GAS) in the promoters of IFN-γ-responsive genes, which triggers the start of transcription (Darnell et al., 1994).

The genes stimulated by IFN-γ via the JAK-STAT pathway produce a wide range of proteins that play a role in antimicrobial defense, antigen processing and presentation, regulation of the cell cycle, programmed cell death, and the activation of different immune system cells, such as macrophages, T cells, and NK cells (Boehm et al., 1997). IFN-γ and the JAK-STAT pathway have a role in infection and cancer, as well as in creating immune responses unique to different tissues and maintaining a balanced immune system. IFN-γ has a significant impact on the differentiation of T helper cells. It promotes the growth and function of Th1 cells while inhibiting the proliferation of Th2 and Th17 cells (Schroder et al., 2004). As a result, it plays a crucial role in determining the outcome of immune responses. Additionally, IFN-γ has the capacity to regulate the activity of different immune cells, such as dendritic cells, B cells, and regulatory T cells, which highlights its adaptable function within the immune system (Schroder et al., 2004). IFN-γ also activates macrophages, improving their ability to engulf foreign particles, increasing the presence of major histocompatibility complex (MHC) molecules, and stimulating the production of reactive oxygen and nitrogen species. These processes are essential for controlling and eliminating intracellular pathogens (Schroder et al., 2004).

IFN-γ regulates the JAK-STAT pathway at several levels to prevent abnormal or extended activation, which may result in pathogenic diseases. Suppressors of cytokine signaling (SOCS) proteins, protein inhibitors of activated STATs (PIAS), and tyrosine phosphatases are examples of negative regulators (Shuai & Liu, 2003; Schroder et al., 2004). These proteins play a role in ensuring that the activation of STAT1 is temporary and dependent on the environment. Such regulation helps to finely adjust the cellular response to IFN-γ. The significance of this control is emphasized in illnesses characterized by dysregulation of IFN-γ signaling. Chronic activation of the IFN-γ JAK-STAT pathway is involved in the development of several autoimmune and inflammatory disorders, such as severe combined immunodeficiency, Crohn's disease, atopic dermatitis and asthma. In these conditions, the excessive and continuous signaling of IFN-γ leads to tissue damage and the progression of the illness (Shuai & Liu, 2003). Furthermore, IFN-γ has the ability to directly inhibit the growth of tumor cells and promote their programmed cell death (Kaplan et al., 1998). It can also increase the ability of tumors to be recognized by the immune system by increasing the production of MHC molecules, which helps in presenting tumor antigens to T cells. However, persistent IFN-γ signaling within the tumor microenvironment might facilitate immune evasion by stimulating the production of immune

checkpoint markers, such as PD-L1, on tumor cells, and by fostering the creation of an immunosuppressive setting (Munn & Bronte, 2016; Yi et al., 2021).

Furthermore, although not directly activated by TNF-α, STAT1 is required for TNF-α-induced apoptosis (Kumar et al., 1997). SOCS1 mediates this cross-talk by inhibiting both NF-κB and STAT1 activation in response to LPS in macrophages (Kinjyo et al., 2002). The interaction of SOCS1 with IL-1R-associated kinase (IRAK) further explains its inhibitory role in NF-κB signaling (Nakagaawa et al., 2002). Thus, SOCS1 links the JAK-STAT and NF-κB pathways, further emphasizing the roles of TNF-α and IFN-γ in immune responses (Shuai & Liu, 2003). Deregulation of JAK-STAT and NF-κB, as well as mutations in some genes activated by those pathways, such as *REL, PDL1,* and *CXCL10,* are considered to be hallmark features of primary mediastinal B-cell lymphoma (PMBCL) (Weniger et al., 2007; Steidl & Gascoyne, 2011).

1.4. Transcription factor cREL

Out of five members of the NF-κB family, reticuloendotheliosis viral oncogene homolog (cREL) has the most significant association with human lymphoma. It plays a pivotal role in the pathogenesis and progression of PMBCL. Characterized by frequent genetic aberrations, including amplifications at the *REL* gene locus, cREL contributes significantly to lymphomagenesis through its transcriptional control over genes that regulate cell survival, proliferation, and immune responses. In PMBCL, these genetic alterations can lead to the constitutive activation of *REL*, promoting tumor growth and survival by enhancing inflammatory pathways and immune evasion mechanisms (Kober-Hasslacher & Schmidt-Supprian, 2019).

1.5. Chemokine CXCL10

Chemokine CXCL10, also known as γ interferon-inducible cytokine 10 (IP-10) (Luster & Ravetch, 1987; Kaplan et al., 1987), recruits T lymphocytes expressing CXCR3, enabling their infiltration into the tumor site. This process is crucial for starting immune responses that effectively target tumor cells. The activation of CXCL10 in PMBCL is important because it stimulates the recruitment of effector T cells that can carry out anti-tumor actions, hence improving immune surveillance and possibly inhibiting tumor development. Furthermore, the capacity of CXCL10 to control the polarization of T cells in the tumor microenvironment not only aids in direct anti-tumor actions but also influences the immune landscape. This functional spectrum emphasizes the possibility of using CXCL10-mediated pathways as a treatment

strategy in PMBCL with the goal of improving T cell-mediated immunity and disrupting the TME's tumor-supportive environment (Karin & Razon, 2018).

1.6. Programmed death receptor 1 and its ligands

Predominantly active in the tumor microenvironment, PD-1 and its ligands, PD-L1 and PD-L2, are expressed by tumor and immune cells, weakening immune response particularly when upregulated by IFN-γ. PD-1 also affects B cells and NK cells, leading to further immunological suppression. Studies including PD-1 inhibitors such as nivolumab show promising results in the treatment of advanced tumors and B-cell malignancies, indicating the important function of PD-1 in immune regulation and cancer therapy (Nicholas et al., 2016; Yi et al., 2021). Extensive research has been done on the role of PD-L1 and its genetic changes in PMBCLthat showed notable clinical effects (Xie et al., 2019).

1.7. Primary mediastinal B-cell lymphoma

PMBCL is a distinct subtype of B-cell lymphoma. Although previously considered a subtype of diffuse large B-cell lymphoma (DLBCL), recent classifications recognize PMBCL as a separate entity. This lymphoma shares clinical and morphological characteristics with both DLBCL and classical Hodgkin lymphoma (cHL), complicating its diagnosis (Campo et al., 2011; Lees et al, 2019). Standard immunohistochemical biomarkers for PMBCL, such as CD23 and MAL, can assist in differentiation from DLBCL and nodular sclerosis Hodgkin lymphoma (NScHL), but these markers are not without limitations. Advanced diagnostic techniques like genetic profiling and molecular studies are being used to improve diagnostic accuracy and tailor therapeutic strategies (Steidl et al., 2011; Lees et al., 2019).

PMBCL, which mostly originates in the mediastinum, commonly occurs in young adults, especially females, and usually shows local invasion. Clinically, PMBCL commonly affects women in their 30s and 40s and often presents with compressive symptoms due to a large mediastinal mass. Superior vena cava obstruction is common, and while initial disease tends to be localized, relapse can lead to widespread dissemination. Pathologically, PMBCL exhibits genetic markers of germinal center transit, consistent with its origin from thymic B-cells (Lees et al., 2019).

Genetically, PMBCL is marked by frequent amplifications of chromosome 9p24.1, leading to the overexpression of *JAK2*, *JMJD2C*, and *PDL1*/*PDL2* genes. This results in the constitutive activation of the JAK-STAT and NF-κB signaling pathways. *REL* gene is often amplified, resulting in nuclear localization of cREL and increased NF-κB pathway activity (Weniger et al.,

2007; Steidl & Gascoyne, 2011). The *REL* gene is located on chromosome 2p12-16. According to Kober-Hasslacher & Schmidt-Supprian (2019), chromosomal 2p overrepresentations in PMBCL occur in 28% of cases on average. Bea et al. (2005) found 2p gains in 47% of samples and Lenz et al. (2008) reported 26% with gains and 19% with amplifications, based mostly on the same cohort. An independent cohort showed 2p gains in 27% of biopsies, including some with high-level *REL* amplifications (Joos et al., 1996). Comparative genomic hybridization (CGH) by Bentz et al. (2001) identified 2p14-16 overrepresentation in 19% of cases, and Weniger et al. (2007) using fluorescence in situ hybridization (FISH) confirmed additional gains and amplifications, totaling 15 *REL* copy number changes in 20 samples. The constitutive activation of NF-κB is frequently caused by amplifications of the *REL* gene and mutations in *TNFAIP3* gene, which encodes tumor necrosis factor alpha-induced protein 3 (TNFAIP3), a negative regulator of the pathway. Aside from the amplification of 9p24.1, there are also common mutations in *SOCS1* and *STAT6* that contribute to the dysregulation of JAK/STAT signaling. Altered histone modification is also involved, since the overexpression of *JMJD2C* results in abnormal methylation of histone 3, which in turn promotes the development of active chromatin (Lees et al., 2019; Steidl & Gascoyne, 2011).

PMBCL has the ability to evade the immune system through many different strategies, including the suppression of MHC class II molecules and the overproduction of PD-1 ligands. For example, Twa et al. (2014) found frequent rearrangements of 9p24.1 in PMBCL, with break-apart occurring in about 20% of cases and amplification in 29%, and Shi et al. (2014) observed elevated PD-L2 protein expression in the majority of PMBCL cases (72%), contrasting with its rare expression in DLBCL (3%), often associated with *PDCD1LG2* copy gain. Genetic changes affecting *CIITA*, the master regulator of MHC class II genes, are also common in PMBCL and result in decreased MHC class II expression. Steidl et al. (2011) identified recurrent breaks of the *CIITA* gene in 38% of PMBCL cases, compared to 15% in classical Hodgkin lymphoma (cHL). Additionally, Roberts et al. (2006) linked poor patient survival in PMBCL to decreased MHC II expression. The reduction in MHC II expression combined with the increased production of PD-1 ligands allows PMBCL cells to evade immune surveillance (Lees et al., 2019).

Research of PMBCL involves a combination of several different approaches and advanced molecular techniques to create a comprehensive picture of this type of lymphoma. For example, in vitro studies, use cell lines derived from PMBCL as a model to investigate its molecular mechanisms, genetic profile and responses to various types of therapy. Most commonly used

cell lines are MedB-1, Karpas 1106p, Farage and U-2940 (Dai et al., 2015. These cell lines are also used to study tumor growth, metastasis, and therapeutic efficacy in a live organism by implanting them as xenografts into immunodefficient mice (Hao et al., 2014; Lee et al., 2018). Lastly, clinical trials provide invaluable insights by correlating molecular findings with patient outcomes, assessing the efficacy and safety of novel therapeutic interventions, and identifying potential biomarkers for prognosis and treatment response (Zinzani et al., 2019).

1.8. Cervical carcinoma

Cervical carcinoma is one of the most common carcinomas affecting women worldwide. In contrast to PMBCL, cervical carcinoma relies less on the activation of JAK-STAT and NF-κB pathways. It is mostly caused by an infection with high-risk types of human papillomavirus (HPV), namely HPV-16 and HPV-18 (Walboomers et al., 1999; Schiffman et al., 2011). These viruses integrate their DNA into the host genome, which causes the disruption of normal cellular functions. However, multiple genetic and epigenetic changes must occur in order for HPV infection to progress to cervical carcinoma. HPV oncoproteins E6 and E7 inactivate tumor suppressor proteins p53 and retinoblastoma (Rb), respectively. This inactivation disrupts cell cycle regulation and promotes genomic instability. These changes result in uncontrolled cell proliferation, resistance to apoptosis, and increased potential for metastasis. The pathology of cervical carcinoma typically begins with pre-cancerous lesions known as cervical intraepithelial neoplasia (CIN), which can progress to invasive carcinoma if left untreated (Schiffman et al., 2011). In addition to these viral oncoproteins, cervical carcinoma cells often exhibit mutations in various other genes, some involved in DNA repair, such as *BRCA1* and *BRCA2*, further contributing to genetic instability (Charo & Keating, 2005; Cancer Genome Atlas Research Network, 2017).

Similarly to PMBCL, cervical cancer research involves a combination of experimental and clinical approaches to unravel the complexities of the disease, with a particular focus on the role of HPV in its pathogenesis. Common cervical cancer cell lines such as HeLa, SiHa, and CaSki are utilized in vitro and in vivo to explore the genetic alterations, molecular pathways, and therapeutic responses (Meissner, 1999; Zheng et al., 2021). Another critical in vivo approach involves patient-derived xenografts (PDX), where tumor samples from cervical carcinoma patients are implanted into mice, preserving the tumor's original genetic and phenotypic traits (Tanaka et al., 2021). Clinical studies linking laboratory findings with patient care also play an important role in our understanding of this type of cancer (Schmidt et al., 2022).

2. Research objectives

The objective of this research is to analyze the expression of the *REL*, *PDL1* and *CXCL10* genes after treatment with tumor necrosis factor α (TNF-α) and the *CXCL10* and *PDL1* genes after treatment with interferon γ (IFN-γ) in cell lines of lymphoid origin MedB-1 (Möller et al., 2001) and Karpas 1106p (Nacheva et al., 1994) and in the epithelial cell line HeLa in order to determine whether these cytokines equally affect tumors originating from epithelial and lymphoid cells. The research hypothesis is that tumor cells of different origins, due to variations in the number of copies of certain genes and unique expression patterns, will show different responses to treatment with cytokines TNF-α and IFN-γ, depending on the concentration of cytokines.

3. Materials and methods

3.1 Materials

In this study I have used cell pellets from the lymphoid-origin cell lines MedB-1 and Karpas 1106p, as well as the epithelial-origin cell line HeLa. The cells have been previously treated with the cytokine TNF-α (5, 10, 20, and 50 ng/ml) and cytokine IFN-γ (30 and 50 ng/ml) for 24 and 48 hours. Control cells were not given any treatment. Each experiment was performed in triplicate.

This research would not have been possible without the support of Dr. K. Mellert, Dr. S. Bruderlein and Prof. Dr. P. Möller whom we are very grateful for providing the cell line MedB-1. Möller et al. (2001) established MedB-1 cell line using tumor tissue from a 27-year-old male patient with PMBCL, presented with a large lump in the anterior part of the chest. MedB-1 not only has a similar immunophenotypic profile to the parental tumor, but it also has the same cytogenetic abnormalities, namely affecting chromosomes X and 9, which are known to have a role in the development of PMBCL. The cell line shows gains in genetic material on chromosome 9p, particularly in the area where the *JAK2* gene is located.

The Karpas 1106p cell line, derived from a 23-year-old woman with mediastinal lymphoblastic B-cell non-Hodgkin's lymphoma (B-NHL) (Nacheva et al. 1994), is characterized by its unique chromosomal abnormality. It has a complex translocation affecting chromosome 18q21.3, linked to various B-cell lymphomas. Karpas 1106 also exhibits characteristics of mature B-cells, expressing IgG and lacking BCL2 protein. The complex karyotype includes additional chromosomal abnormalities, such as deletions and rearrangements, which may contribute to the aggressive nature of the original tumor. The Karpas 1106 line showed 4 times greater NF-κB activity compared to the DHL6 cell line, suggesting constitutive activation of NF-κB pathway (Feuerhake et al. 2005).

HeLa cell line, isolated in 1951 from cervical cancer tissue from a 31-year-old female patient, is the first cultivated human cell line (Gey et al. 1952; Masters 2002). Its number of chromosomes ranges between 70 and 164, with the modal number of 82 (Chen, 1988). The cells show positivity for keratin when tested with immunoperoxidase staining. HeLa cells have been documented to carry sequences of HPV-18 (Pater & Pater, 1985). Additionally, p53 expression was observed to be low, while normal levels of the retinoblastoma suppressor protein (pRB) were detected. Transcriptome analysis of HeLa cells found that around 2000 genes are expressed at levels higher than those observed in 16 different human tissues. The primary role

of these genes is mostly related to processes such as cell proliferation, transcription, and DNA repair (Landry et al. 2013).

3.2. Methods

3.2.1. RNA isolation and quality control

I have extracted the total RNA from the cell pellets using the Quick-DNA/RNA FFPE MiniPrep Kit (Zymo Research, Irvine, CA, USA). Deparaffination and tissue digestion steps were skipped and cell pelets were incubated in 600 µL of DNA/RNA Lysis Buffer for 1 minute at room temperature. RNA isolation was further done according to the manufacturer's instructions. Following the isolation, I assessed the RNA quantity and quality using spectrophotometer NanoVue (Thermo Fisher Scientific, USA) (Shen 2019).

3.2.2. cDNA synthesis

I performed reverse transcription of the purified RNA to complementary DNA (cDNA) using the PrimeScript Reverse Transcriptase kit (Takara, Kusatsu, Japan), DNTPs (Sigma Aldrich, St. Louis, Missouri, USA), RNase-free water (Lonza Group, Basel, Switzerland), and random hexamers (Invitrogen, Waltham, Massachusetts, USA). I prepared two reaction mixtures in microcentrifuge tubes according to Table 1. I calculated the volume of the RNA template to be added to the first reaction mixture using the concentrations of the isolated RNA, so that the total mass of RNA added did not exceed 500 ng. After adding the calculated volume of the RNA template to the reaction mixture, I added RNase-free water to the sample to reach a total volume of 10 µL. For samples with lower concentrations, I added the RNA template in a volume of 8 µL, without the RNase-free water. For the positive control, I added 120-160 ng of RNA template isolated from fresh cells of lymphoid origin and supplemented it with RNase-free water to the final volume. In order to eliminate the possibility of contamination, I used 8 µL of RNase-free water instead of RNA in the negative control reactions. The samples were then incubated for 5 minutes at 65°C to denature the RNA, then quickly cooled on ice for at least 5 minutes. While the first reaction mixture was incubating, I prepared the second reaction mixture. The reaction mixture was then incubated according to the protocol: 10 minutes at 30°C, 60 minutes at 42°C, and 15 minutes at 70°C, followed by holding at 4°C indefinitely. The generated cDNA was stored at a temperature of -20°C.

Table 1. Reverse transcription reaction mixtures.

Reaction mix	**Ingredients**	**Final concentration**
Mixture I	Random hexamers (50 µM) (Invitrogen, USA)	5 µM
	Deoxyribonucleotide mix (10 mM) (Sigma Aldrich, USA)	1 mM
	RNA	≤ 500 ng
	AccuGene water (Lonza Group, Switzerland)	up to 10 µL
	Total volume	**10 µL**
Mixture II	Mixture I	
	5x PSRT buffer (Takara, Japan)	1X
	PrimeScript Reverse Transcriptase (200 U/µL) (Takara, Japan)	5 U/µL
	Recombinant RNase inhibitor (40 U/µL) (Takara, Japan)	1 U/µL
	AccuGene water (Lonza Group, Switzerland)	up to 20 µL
	Total volume	**20 µL**

3.2.3. Quantitative Real-Time PCR

I have measured the expression levels of the target genes *REL*, *PDL1*, and *CXCL10* using real-time polymerase chain reaction (RT-PCR), which was carried out using the PowerUp SYBR Green Master Mix (Applied Biosystems, Waltham, Massachusetts, USA). I used *HPRT1* gene as endogenous control, and specific primers listed in Table 2 for analyzed genes.

Table 2. Primer sequences for the genes *REL*, *CXCL10*, *PD-L1*, and *HPRT1*.

Gene	Primer orientation	Primer sequence
REL	Forward	5'-GAACCCAATTTATGACAACCGTGC-3'
	Reverse	5'-TTTCATCTCCTCCTCTGACACTTC-3'
CXCL10	Forward	5'-AAAGCAGTTAGCAAGGAAAGGTCT-3'
	Reverse	5'-CTGTGTGGTCCATCCTTGGAA-3'
PD-L1	Forward	5'-GGGCATTCCAGAAAGATGAGGA-3'
	Reverse	5'-AACCGTGACAGTAAATGCGTTC-3'
HPRT1	Forward	5'-CCTGGCGTCGTGATTAGTGAT-3'
	Reverse	5'-AGACGTTCAGTCCTGTCCATAA-3'

I prepared the reaction mixtures for individual genes in microcentrifuge tubes according to Table 3. I calculated the volume of the cDNA template based on the concentration of the isolated RNA and the assumed cDNA concentration of 500 ng/20 µl. I added the cDNA template so that the total amount of cDNA per well did not exceed 50 ng. I also prepared three controls: a positive qPCR control, a negative qPCR control, and a negative reverse transcription control. For the positive qPCR control, I added 1 µl of the cDNA made from RNA template used as a positive control for reverse transcription and supplemented it with water to the final volume. For the negative qPCR control, I only added water to the final volume, and for the reverse transcription control, I added 1 µl of the negative reverse transcription control and water to the final volume. Each PCR reaction was run in duplicate, including no-template controls. The reactions were run according to the protocol: 2 minutes at 50°C, 10 minutes at 95°C, and 40 cycles of 15 seconds at 95°C for DNA denaturation followed by 1 minute at 95°C for primer alignment and amplification. The amplification data were collected and analyzed using the CFX96 Real-Time System (Bio-Rad, Hercules, California, USA).

Table 3. Real-time polymerase chain reaction mastermix.

Ingredients	Final concentrations
2X SYBR Green PCR Master Mix (Applied Biosystems, USA)	1X
Forward primer (10 µM)	0,05 µM
Reverse primer (10 µM)	0,05 µM
cDNA	< 50 ng
AccuGene water (Lonza Group, Switzerland)	up to 20 µL
Total volume	**20 µL**

3.2.4. Data quantification and normalization

I have quantified the relative gene expression levels based on the cycle threshold (Ct) values, which inversely correlate with the amount of target nucleic acid in the sample, using the delta-delta Ct (ddCt) method (Livak & Schmittgen, 2001). This approach involved normalizing the Ct values of target genes to the endogenous control, *HPRT1*, to account for any sample-to-sample variations. I calculated the normalized Ct values (dCt) for each triplicate, then calculated the ddCt value using the following formula: ddCt = average dCt(treated) – average dCt(untreated). Finally, I calculated the fold change in gene expression (FC) across different cell lines and experiment conditions using the formula: $FC = 2^{-ddCt}$.

Additionally, to facilitate a relative comparison of gene expression between the lymphoid and epithelial cell lines in response to cytokine treatment, I have utilized a HeLa-Normalized Fold Change (HFC) metric. This normalization technique entailed adjusting the average dCt values of the MedB-1 and Karpas 1106p cell lines with those from the HeLa cell line, which served as a constant reference across all experiments. The HFC was calculated using the formula: $HFC = 2^{[\text{average dCt(Cell Line)} - \text{average dCt(HeLa)}]}$, thus enabling a direct comparison of gene expression changes relative to the baseline established by HeLa cells.

3.2.5. Statistical analysis

Differences in gene expression levels between treatments and cell lines were statistically evaluated using an independent variables t-test, which I have conducted using the Microsoft Excel. Significant level was set at a p-value threshold of less than 0.05 after Benjamini-Hochberg correction for multiple testing.

4. Results

4.1. RNA isolation

4.1.1. MedB-1 cell line

At 24 hours post-treatment, RNA concentrations in MedB-1 cells treated with TNF-α and IFN-γ ranged from 53.6 to 200.4 µg/ml. Most samples showed high purity with $A_{260/280}$ ratios near 2.0 and $A_{260/230}$ ratios for most samples were above 2.0, with some deviations below this threshold (Table 4). After 48 hours, RNA concentrations increased considerably (up to 315.2 µg/ml) with better purity ratios overall (Table 5).

Table 4. Concentrations and purity of RNA isolated from the pellets of fresh MedB-1 cells 24 hours after treatments with TNF-α (5, 10, 20, and 50 ng/ml) and IFN-γ (30 and 50 ng/ml). NT - untreated samples, PC - positive control

MedB-1				
24 h post-treatment				
Treatment	**Sample**	**γ(RNA) / µg ml^{-1}**	**$A_{260/280}$**	**$A_{260/230}$**
TNF-α 5 ng ml^{-1}	a	118.4	2.041	2.295
	b	160.0	2.051	2.353
	c	185.2	2.031	2.281
TNF-α 10 ng ml^{-1}	a	157.6	2.052	1.807
	b	127.6	2.045	0.786
	c	84.8	2.000	1.696
TNF-α 20 ng ml^{-1}	a	163.6	2.035	2.351
	b	169.2	2.043	2.074
	c	162.8	2.045	2.261
TNF-α 50 ng ml^{-1}	a	153.6	2.065	1.662
	b	174.4	2.028	2.259
	c	143.6	2.028	2.442
IFN-γ 30 ng ml^{-1}	a	109.6	2.045	2.322
	b	200.4	2.045	2.298
	c	70.8	2.011	1.229
IFN-γ 50 ng ml^{-1}	a	85.2	2.009	2.393
	b	123.2	2.053	2.124
	c	86.0	2.048	2.590
NT	a	53.6	2.030	2.913
	b	155.6	2.047	2.401
	c	160.0	2.041	2.424
PC		39.6	1.980	1.707

Table 5. Concentrations and purity of RNA isolated from the pellets of fresh MedB-1 cells 48 hours after treatments with TNF-α (5, 10, 20, and 50 ng/ml) and IFN-γ (30 and 50 ng/ml). NT - untreated samples, PC - positive control

MedB-1				
48 h post-treatment				
Treatment	**Sample**	**γ(RNA) / µg ml^{-1}**	**$A_{260/280}$**	**$A_{260/230}$**
TNF-α 5 ng ml^{-1}	a	197.2	2.089	1.318
	b	180.0	2.064	1.515
	c	236.8	2.099	1.922
TNF-α 10 ng ml^{-1}	a	179.2	2.074	1.322
	b	182.0	2.078	2.040
	c	131.6	2.056	
TNF-α 20 ng ml^{-1}	a	186.0	2.085	1.615
	b	315.2	2.074	2.101
	c	262.0	2.073	2.198
TNF-α 50 ng ml^{-1}	a	207.6	2.076	2.136
	b	174.8	2.061	2.142
	c	117.6	2.042	2.056
IFN-γ 30 ng ml^{-1}	a	192.8	2.060	2.152
	b	173.6	2.067	2.226
	c	218.4	2.060	2.202
IFN-γ 50 ng ml^{-1}	a	212.0	2.054	2.275
	b	167.2	2.049	2.322
	c	234.0	2.053	2.267
NT	a	127.6	2.071	2.200
	b	213.6	2.054	2.302
	c	259.2	2.064	2.104
PC		32.4	2.025	2.746

4.1.2. Karpas 1106p cell line

At 24 hours post-treatment, RNA concentrations in Karpas 1106p cells treated with TNF-α and IFN-γ ranged from 32.0 to 127.2 μg/ml. The majority of the samples showed good purity, as indicated by $A_{260/280}$ ratios that were typically close to 2.0, with the exception of a few samples (Table 6). After 48 hours, the minimum RNA concentration was 38.4 μg/ml, and the maximum was 108.8 μg/ml. Additionally, there was a general improvement in the overall purity ratios, as seen in Table 7.

Table 6. Concentrations and purity of RNA isolated from the pellets of fresh Karpas 1106p cells 24 hours after treatments with TNF-α (5, 10, 20, and 50 ng/ml) and IFN-γ (30 and 50 ng/ml). NT - untreated samples, PC - positive control

Karpas 1106p				
24 h post-treatment				
Treatment	**Sample**	**γ(RNA) / μg ml^{-1}**	**$A_{260/280}$**	**$A_{260/230}$**
TNF-α 5 ng ml^{-1}	a	51.2	2.065	0.871
	b	60.8	1.974	0.741
	c	127.2	1.395	1.536
TNF-α 10 ng ml^{-1}	a	42.4	1.767	1.710
	b	40.8	1.594	0.694
	c	55.2	1.605	2.604
TNF-α 20 ng ml^{-1}	a	48.4	1.635	0.840
	b	58.4	1.678	2.607
	c	47.6	1.630	3.051
TNF-α 50 ng ml^{-1}	a	47.2	1.639	0.432
	b	32.0	1.538	3.239
	c	48.4	1.658	1.142
IFN-γ 30 ng ml^{-1}	a	77.2	1.787	2.144
	b	69.6	1.812	2.203
	c	64.4	1.713	2.268
IFN-γ 50 ng ml^{-1}	a	59.2	1.682	2.596
	b	75.6	1.783	2.487
	c	55.2	1.747	2.760
NT	a	59.6	1.774	2.403
	b	57.2	1.765	2.860
	c	58.0	1.768	2.788
PC		20.8	1.444	3.023

Table 7. Concentrations and purity of RNA isolated from the pellets of fresh Karpas 1106p cells 48 hours after treatments with TNF-α (5, 10, 20, and 50 ng/ml) and IFN-γ (30 and 50 ng/ml). NT - untreated samples

Karpas 1106p				
48 h post-treatment				
Treatment	**Sample**	**γ(RNA) / µg ml^{-1}**	**$A_{260/280}$**	**$A_{260/230}$**
TNF-α 5 ng ml^{-1}	a	48.0	2.069	0.976
	b	55.6	2.044	1.495
	c	52.8	2.062	0.555
TNF-α 10 ng ml^{-1}	a	60.0	2.055	1.393
	b	60.8	2.000	2.027
	c	52.8	2.095	1.148
TNF-α 20 ng ml^{-1}	a	108.8	1.388	1.381
	b	61.6	2.000	1.878
	c	56.0	2.059	0.778
TNF-α 50 ng ml^{-1}	a	64.0	2.000	1.860
	b	52.0	2.000	1.585
	c	56.4	1.986	1.986
IFN-γ 30 ng ml^{-1}	a	85.6	2.019	2.326
	b	96.0	2.017	1.846
	c	103.6	2.023	2.106
IFN-γ 50 ng ml^{-1}	a	101.6	2.000	1.910
	b	108.8	2.015	2.176
	c	71.2	1.914	3.633
NT	a	48.0	1.765	10.300
	b	46.8	2.017	1.918
	c	38.4	2.133	0.513

4.1.3. HeLa cell line

At 24 hours post-treatment, RNA concentrations in HeLa cells treated with TNF-α and IFN-γ ranged from 133.6 to 448.4 µg/ml. Most samples showed high purity with $A_{260/280}$ ratios close to 2.0 and $A_{260/230}$ ratios generally above 2.0, indicating good RNA quality, with a few exceptions showing slight deviations below this threshold (Table 8). In samples collected 48 hours post-treatment, RNA concentrations rose, reaching the highest level at 935.2 µg/ml (Table 9). The purity ratios, as shown by the $A_{260/280}$ and $A_{260/230}$ ratios, typically remained close to 2.0.

Table 8. Concentrations and purity of RNA isolated from the pellets of fresh HeLa cells 24 hours after treatments with TNF-α (5, 10, 20, and 50 ng/ml) and IFN-γ (30 and 50 ng/ml). NT - untreated samples

HeLa				
24 h post-treatment				
Treatment	**Sample**	**γ(RNA) / µg ml^{-1}**	**$A_{260/280}$**	**$A_{260/230}$**
TNF-α 5 ng ml^{-1}	a	370.0	2.074	2.330
	b	411.6	2.066	2.185
	c	413.2	2.070	2.212
TNF-α 10 ng ml^{-1}	a	374.8	2.046	2.184
	b	418.8	2.037	2.390
	c	351.2	2.037	2.212
TNF-α 20 ng ml^{-1}	a	434.8	2.043	2.293
	b	412.4	2.043	2.166
	c	133.6	2.000	2.242
TNF-α 50 ng ml^{-1}	a	354.4	2.037	2.350
	b	268.0	2.030	2.134
	c	395.6	2.039	2.227
IFN-γ 30 ng ml^{-1}	a	448.4	2.061	1.768
	b	290.0	2.048	2.217
	c	353.6	2.032	2.244
IFN-γ 50 ng ml^{-1}	a	288.8	2.022	2.069
	b	293.6	2.028	2.146
	c	259.2	2.031	2.104
NT	a	331.2	2.024	2.226
	b	223.6	2.004	2.227
	c	290.4	2.017	2.234

Table 9. Concentrations and purity of RNA isolated from the pellets of fresh HeLa cells 48 hours after treatments with TNF-α (5, 10, 20, and 50 ng/ml) and IFN-γ (30 and 50 ng/ml). NT - untreated samples

HeLa				
48 h post-treatment				
Treatment	**Sample**	**γ(RNA) / µg ml^{-1}**	**$A_{260/280}$**	**$A_{260/230}$**
TNF-α 5 ng ml^{-1}	a	745.6	2.042	2.248
	b	880.0	2.075	2.340
	c	887.6	2.040	2.257
TNF-α 10 ng ml^{-1}	a	732.0	2.047	2.243
	b	712.4	2.038	2.232
	c	708.8	2.041	2.272
TNF-α 20 ng ml^{-1}	a	544.8	2.024	2.285
	b	894.4	2.048	2.259
	c	935.2	2.045	2.239
TNF-α 50 ng ml^{-1}	a	686.4	2.050	2.206
	b	787.6	2.040	2.253
	c	624.4	2.017	2.369
IFN-γ 30 ng ml^{-1}	a	890.8	2.054	2.268
	b	504.0	2.026	2.382
	c	716.4	2.040	2.279
IFN-γ 50 ng ml^{-1}	a	430.4	2.026	2.242
	b	584.8	2.022	2.409
	c	381.2	2.019	2.296
NT	a	438.8	2.017	2.281
	b	408.4	2.018	2.200
	c	320.8	2.015	2.298

4.2. Changes in gene expression following TNF-α treatment

4.2.1. The analysis of *REL* expression in model cell lines MedB-1, Karpas1106p and HeLa after TNF-α treatment

In the initial 24-hour period post TNF-α treatment, notable differential responses were observed across cell lines for *REL* gene expression (Figure 1.A). Specifically, MedB-1 cells showed statistically significant lower *REL* expression at the 20 ng/ml concentration with a 2.5-fold decrease compared to baseline expression measured in untreated samples. Both Karpas 1106p and HeLa cells did not show significant change in *REL* expression at any of the administered doses.

After 48 hours post-treatment (Figure 1.B), MedB-1 cells showed a dose-dependent increase in *REL* expression at doses of 10, 20, and 50 ng/ml. The Karpas 1106p cells consistently showed no change in expression at all doses, whereas HeLa cells exhibited a significant increase in *REL* expression in comparison to untreated samples only at the dosage of 5 ng/ml, with a fold change of 1.59.

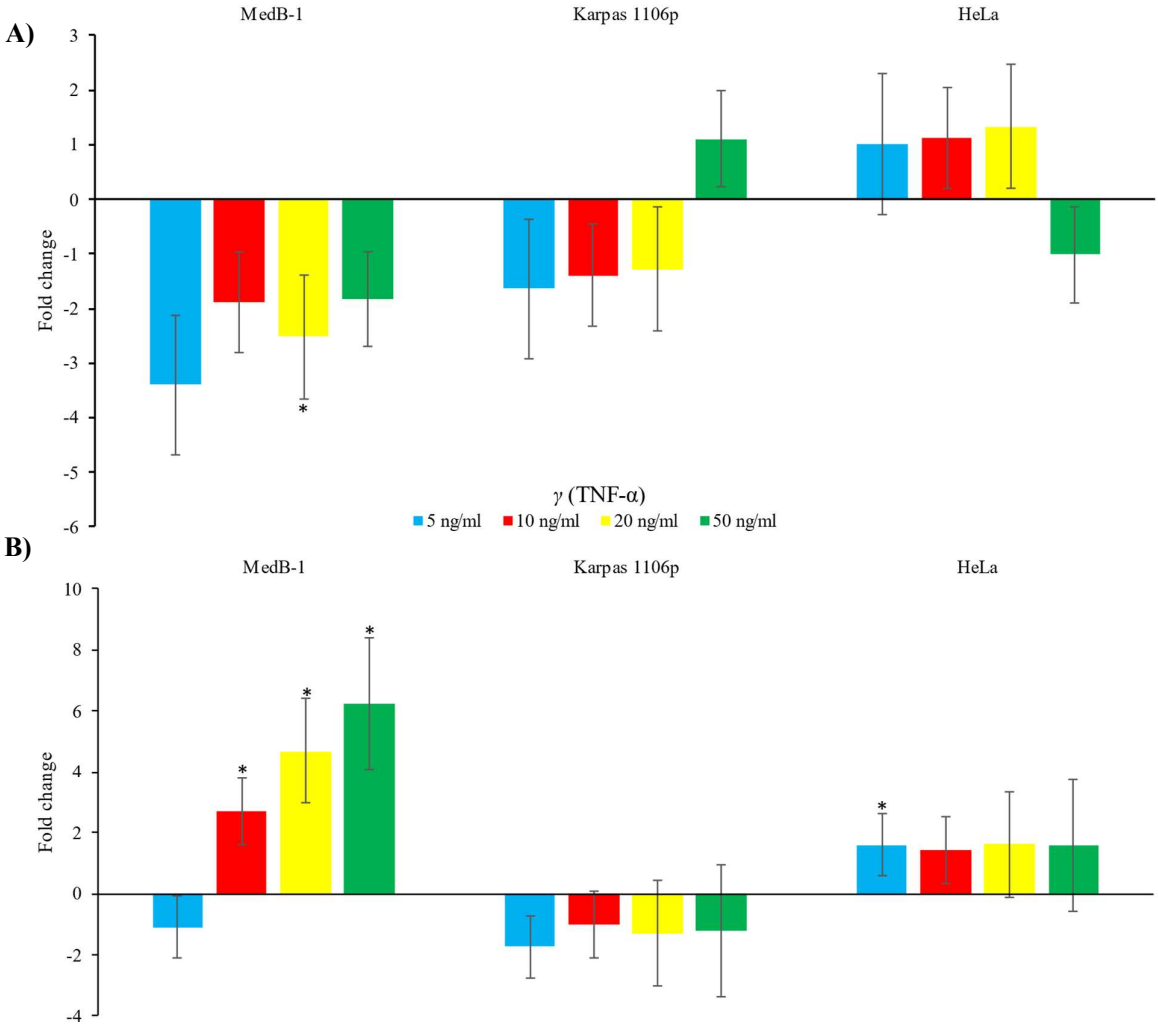

Figure 1. Changes in *cREL* expression across cell lines **A)** 24 hours and **B)** 48 hours post-treatment with 5 ng/ml (blue), 10 ng/ml (red), 20 ng/ml (yellow) and 50 ng/ml (green) of TNF-α. Asterisk (*) marks the statistically significant results determined by independent variable t-test ($p < 0,05$).

4.2.2. The analysis of *CXCL10* expression in model cell lines MedB-1, Karpas1106p and HeLa after TNF-α treatment

In examining the effect of TNF-α on the expression of the *CXCL10* gene, MedB-1 and Karpas 1106p cells showed no change in expression levels at the 24-hour mark for all dosages (Figure

2.A). Contrastingly, HeLa cells presented a clear dose-dependent increase in *CXCL10* expression at 5, 10, and 20 ng/ml compared to untreated cells.

After 48 hours, no statistically significant changes were noted at any dosage in any of the cell lines examined (Figure 2.B).

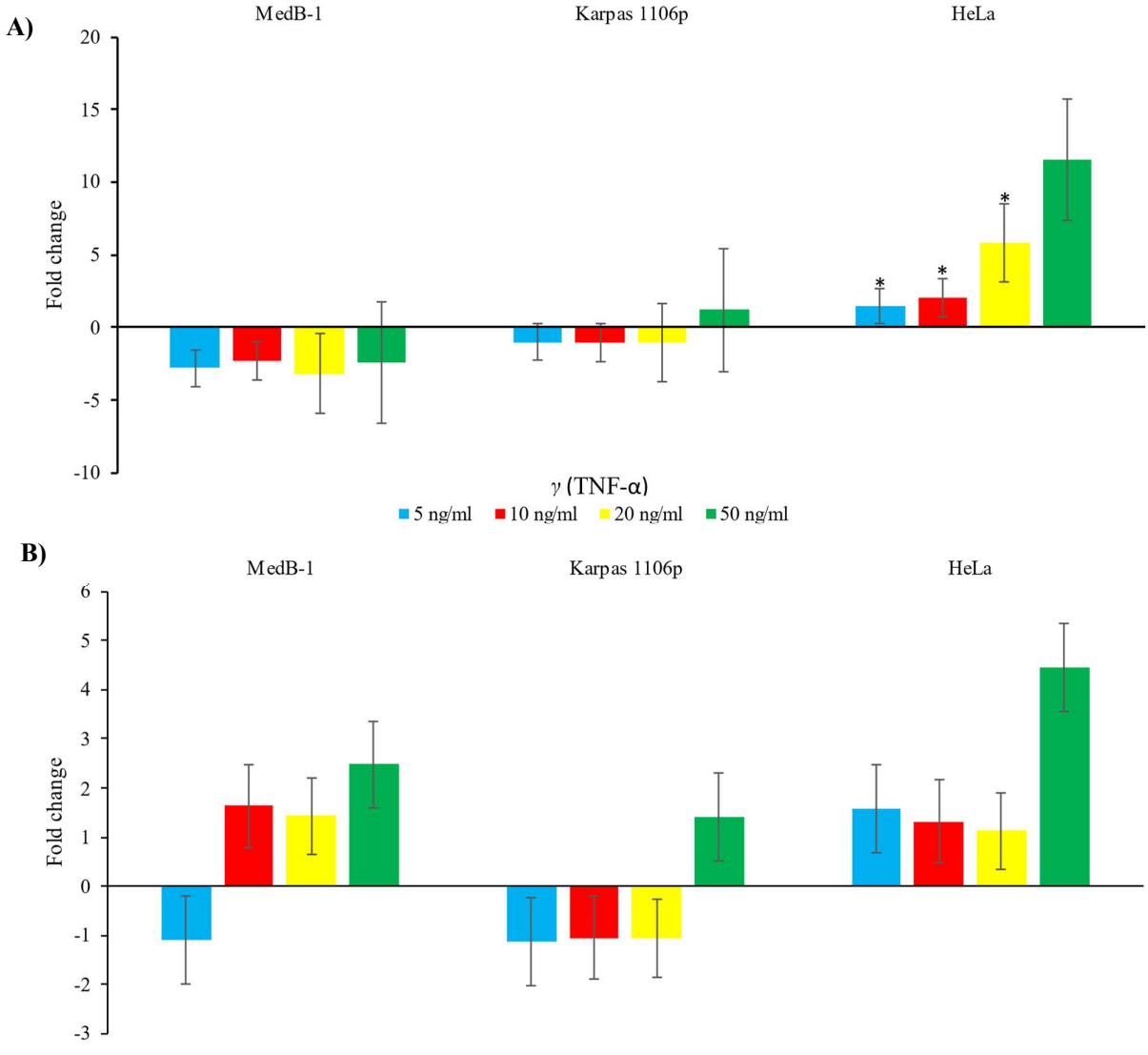

Figure 2. Changes in *CXCL10* expression across cell lines **A)** 24 hours and **B)** 48 hours post-treatment with 5 ng/ml (blue), 10 ng/ml (red), 20 ng/ml (yellow) and 50 ng/ml (green) of TNF-α. Asterisk (*) marks the statistically significant results determined by independent variable t-test ($p < 0,05$).

4.2.3. The analysis of *PDL1* expression in model cell lines MedB-1, Karpas1106p and HeLa after TNF-α treatment

Within 24 hours of TNF-α exposure, MedB-1 cells displayed no statistically significant changes in *PDL1* expression (Figure 3.A). In Karpas 1106p cells, a statistically significant decrease from baseline *PDL1* expression was observed at the 20 ng/ml dose. HeLa cells, conversely, exhibited an increase in *PDL1* expression at the 5 and 50 ng/ml concentrations.

Observing the 48-hour time point (Figure 3.B), MedB-1 cells demonstrated a dose-dependent increase in *PDL1* expression, with statistically significant changes across a range from 10 to 50 ng/ml. Karpas 1106p cells and HeLa cells showed no changes in *PDL1* expression.

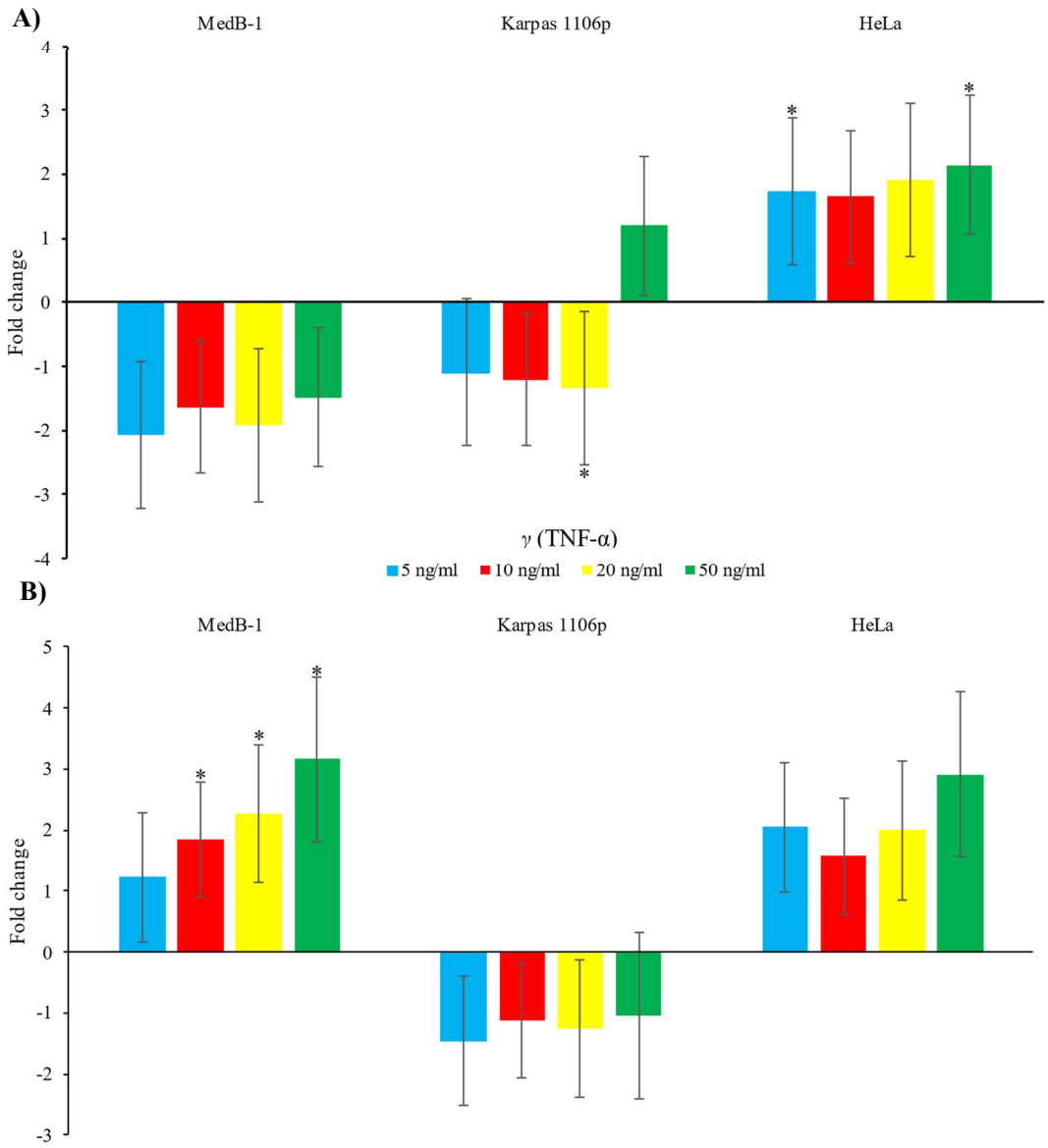

Figure 3. Changes in *PDL1* expression across cell lines **A)** 24 hours and **B)** 48 hours post-treatment with 5 ng/ml (blue), 10 ng/ml (red), 20 ng/ml (yellow) and 50 ng/ml (green) of TNF-α. Asterisk (*) marks the statistically significant results determined by independent variable t-test ($p < 0,05$).

4.3. Changes in gene expression following IFN-γ treatment

4.3.1. The analysis of *CXCL10* expression in model cell lines MedB-1, Karpas1106p and HeLa after IFN-γ treatment

Upon a 24-hour treatment with IFN-γ, an increase in *CXCL10* expression was recorded in MedB-1 and Karpas 1106p cells (Figure 4.A). MedB-1 cells showed a 264-fold rise at 30 ng/ml and a 525-fold increase at 50 ng/ml. Expression of *CXCL10* in Karpas 1106p cells increased 169-fold compared to baseline at 30 ng/ml and 199-fold at 50 ng/ml. HeLa cells did not show statistically significant changes in *CXCL10* expression.

Extending the observation to 48 hours, all cell lines exhibited changes in *CXCL10* expression compared to the untreated groups (Figure 4.B). In MedB-1 cells, *CXCL10* expression increased 1245-fold at 30 ng/ml and 1072-fold at 50 ng/ml. Karpas 1106p cells showed 109-fold increase in *CXCL10* expression at 30 ng/ml and 123-fold at 50 ng/ml. In HeLa cells *CXCL10* expression increased 15-fold at 30 ng/ml and 26-fold at 50 ng/ml.

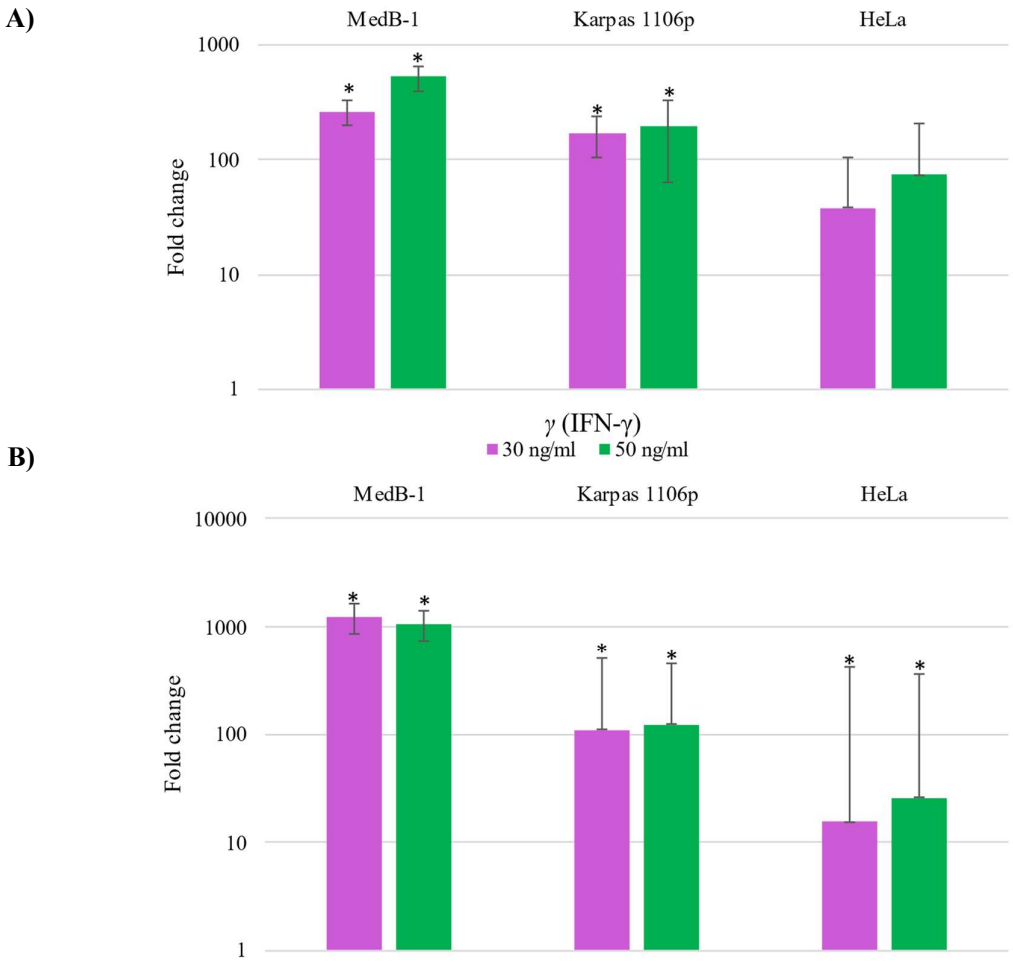

Figure 4. Changes in *CXCL10* expression across cell lines **A)** 24 hours and **B)** 48 hours post-treatment with 30 ng/ml (purple) and 50 ng/ml (green) of IFN-γ. Asterisk (*) marks the statistically significant results determined by independent variable t-test ($p < 0,05$).

4.3.2. The analysis of *PDL1* expression in model cell lines MedB-1, Karpas1106p and HeLa after IFN-γ treatment

In the first 24 hours after IFN-γ treatment, *PDL1* expression in MedB-1 cells did not change (Figure 5.A). Karpas 1106p cells exhibited a 1.6-fold increase in *PDL1* expression at 30 ng/ml and a 1.8-fold at 50 ng/ml. HeLa cells showed significant changes with a 17-fold increase from baseline at 30 ng/ml and a 21-fold increase at 50 ng/ml.

Observations at 48 hours post-treatment (Figure 5.B) revealed that MedB-1 cells had a significant 8-fold increase in *PDL1* expression at 30 ng/ml and a 5-fold increase at 50 ng/ml. Karpas 1106p cells exhibited a 2-fold increase at 30 ng/ml. HeLa cells maintained *PDL1* expression levels recorded at a 24-hour time point at both concentrations.

A)

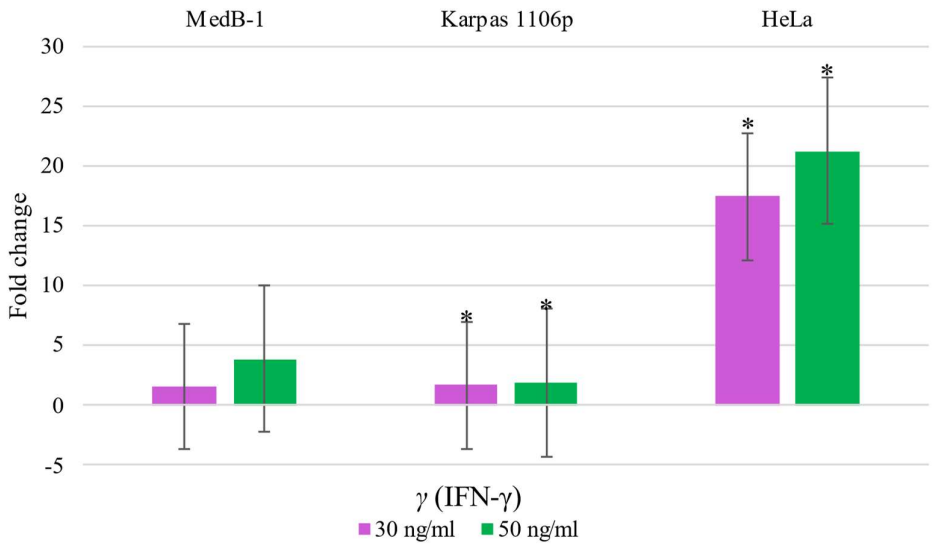

B)

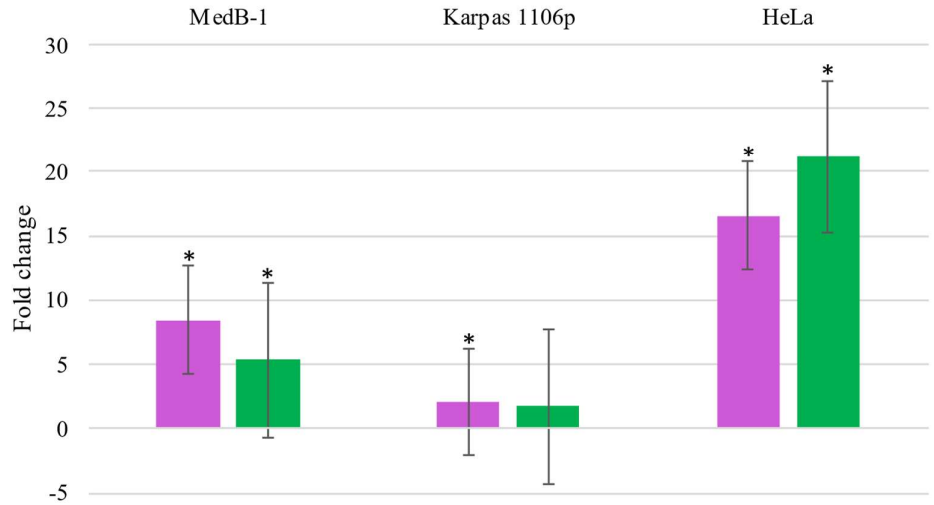

Figure 5. Changes in *PDL1* expression across cell lines **A)** 24 hours and **B)** 48 hours post-treatment with 30 ng/ml (purple) and 50 ng/ml (green) of IFN-γ. Asterisk (*) marks the statistically significant results determined by independent variable t-test ($p < 0,05$).

4.4. Comparison of gene expression between the lymphoid and epithelial cell lines following TNF-α treatment

4.4.1. Comparison of *REL* expression between the lymphoid and epithelial cell lines following TNF-α treatment

At 24 hours post-treatment, MedB-1 cells exhibit a significant reduction in *REL* expression from a baseline HFC of 33, with a notable decrease at the lowest concentration of 5 ng/ml (Figure 6.A). This suppression is lessened at higher concentrations, indicating an initial strong response that partially recovers over time. Conversely, Karpas 1106p cells start with a lower baseline expression (5-fold HFC) and show a moderate and somewhat variable reduction in *REL* expression levels, with no clear dose-dependency observed 24 hours after TNF-α exposure.

Extending the observation to 48 hours, MedB-1 cells display a pronounced dose-dependent increase in *REL* expression, with fold changes rising significantly with higher cytokine concentration (Figure 6.B). In Karpas 1106p cells, the expression of *REL* after 48 hours after treatment increases compared to the 24-hour time point, however the fold changes are smaller and less sensitive to the dosage compared to MedB-1. The data show that there is a change in *REL* expression over time in response to TNF-α in both cell lines. MedB-1 cells show more varied changes in expression at different time points and concentrations, while Karpas 1106p cells have a more stable and consistent expression pattern, both initially and at a later time point.

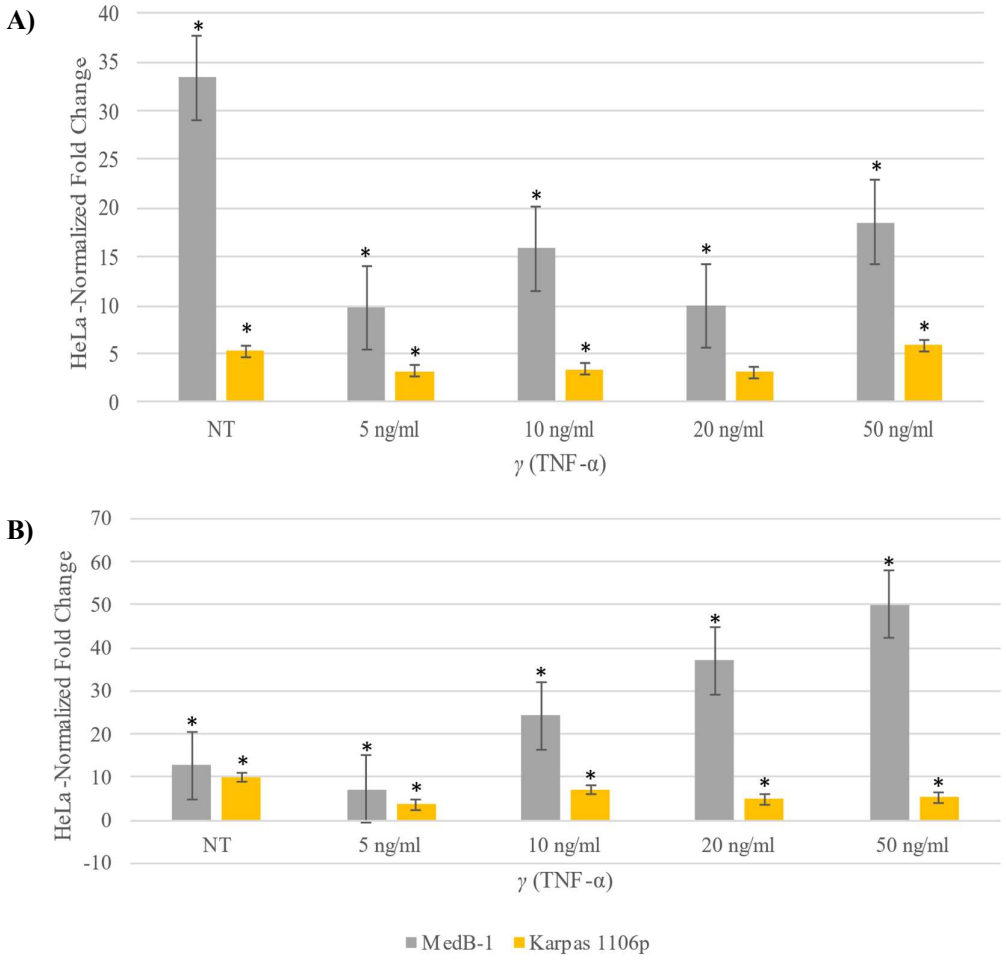

Figure 6. HeLa-normalized fold change in *REL* expression in lymphoid cell lines MedB-1 (grey) and Karpas 1106p (yellow) **A)** 24 hours and **B)** 48 hours post-treatment with increasing concentrations of TNF-α. Asterisk (*) marks the statistically significant results determined by independent variable t-test ($p < 0,05$).

4.4.2. Comparison of *CXCL10* expression between the lymphoid and epithelial cell lines following TNF-α treatment

At 24 hours post-treatment with TNF-α, the HFC data for *CXCL10* expression in MedB-1 cells showed a sharp decrease from baseline level of 1295 HFC (Figure 7.A). This marked reduction continued in a dose-dependent manner, with the highest expression noted at the concentration of 5 ng/ml (317-fold HFC) and the lowest expression at 50 ng/ml (47-fold HFC). In the Karpas 1106p cell line, the baseline level of *CXCL10* expression was around 17.5-fold HFC, and the expression decreased across the gradient of TNF-α concentrations.

Progressing to the 48-hour time point (Figure 7.B), HeLa-normalized fold change of *CXCL10* expression in MedB-1 cells remained above 1000, with no clear pattern, although starting from a higher baseline compared to the 24-hour mark, with HFC of 3393. At concentrations of 10 and 20 ng/ml, HFC even exceeded 4000. The expression in Karpas 1106p cells remained substantially lower than in MedB-1 cells, reaching its highest in untreated cells (HFC of 315) and lowest at 50 ng/ml (HFC of 100).

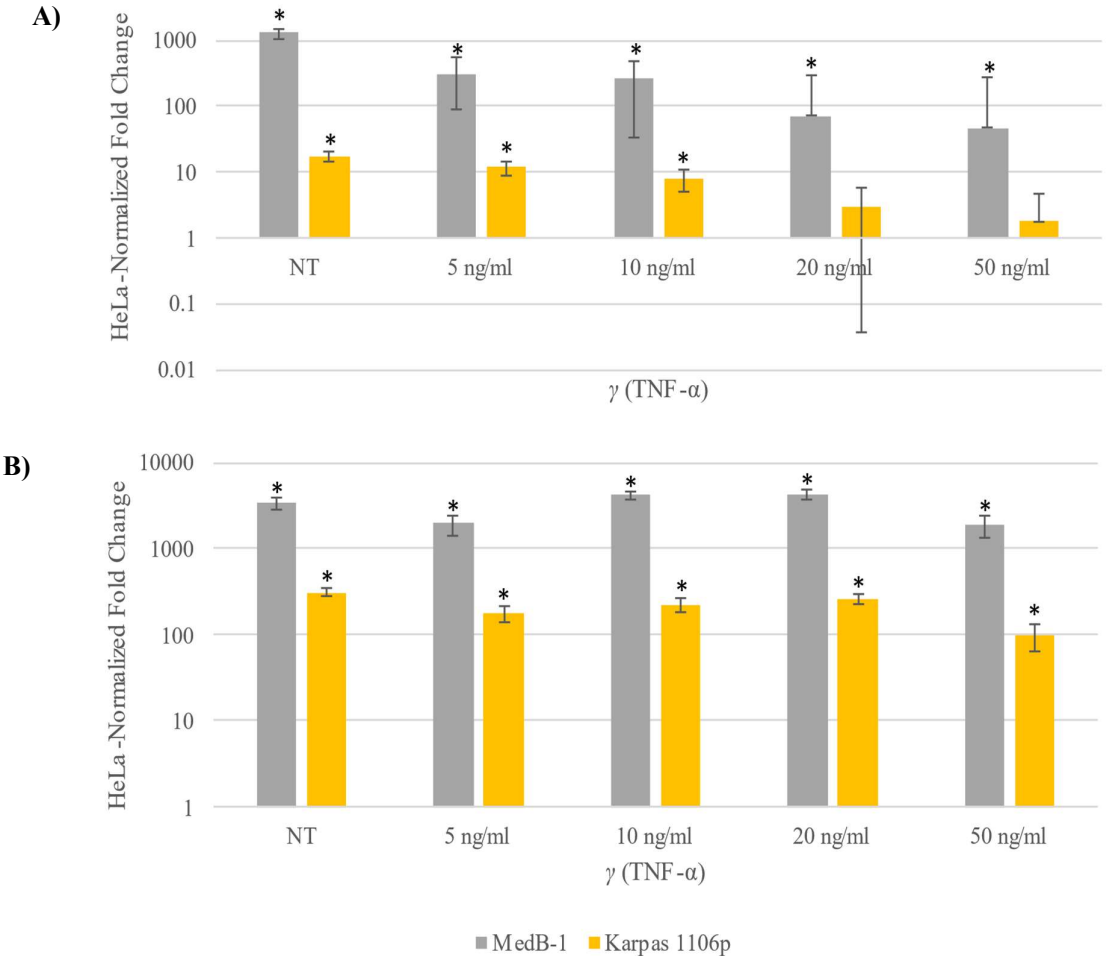

Figure 7. HeLa-normalized fold change in *CXCL10* expression in lymphoid cell lines MedB-1 (grey) and Karpas 1106p (yellow) **A)** 24 hours and **B)** 48 hours post-treatment with increasing concentrations of TNF-α. Asterisk (*) marks the statistically significant results determined by independent variable t-test ($p < 0,05$).

4.4.3. Comparison of *PDL1* expression between the lymphoid and epithelial cell lines following TNF-α treatment

At 24 hours post-treatment with TNF-α, the MedB-1 cell line exhibited a decrease in *PDL1* expression from baseline, with HFC values around 1000 for all doses (Figure 8.A). The Karpas 1106p cell line also showed a decrease in expression from its baseline but maintained a relatively stable expression across the range of TNF-α concentrations.

Progressing to 48 hours post-treatment (Figure 8.B), *PDL1* expression in the MedB-1 cell line showed was lower at the lowest concentration of TNF-α but increased at higher concentrations, with the highest fold change observed at 10 ng/ml. The Karpas 1106p cell line displayed a similar pattern to the 24-hour mark with a decrease at 5 ng/ml and then a rise in expression at higher concentrations. Across both time points, MedB-1 and Karpas 1106p showed a decrease in expression at the lowest concentration of TNF-α, with a varying response at higher concentrations.

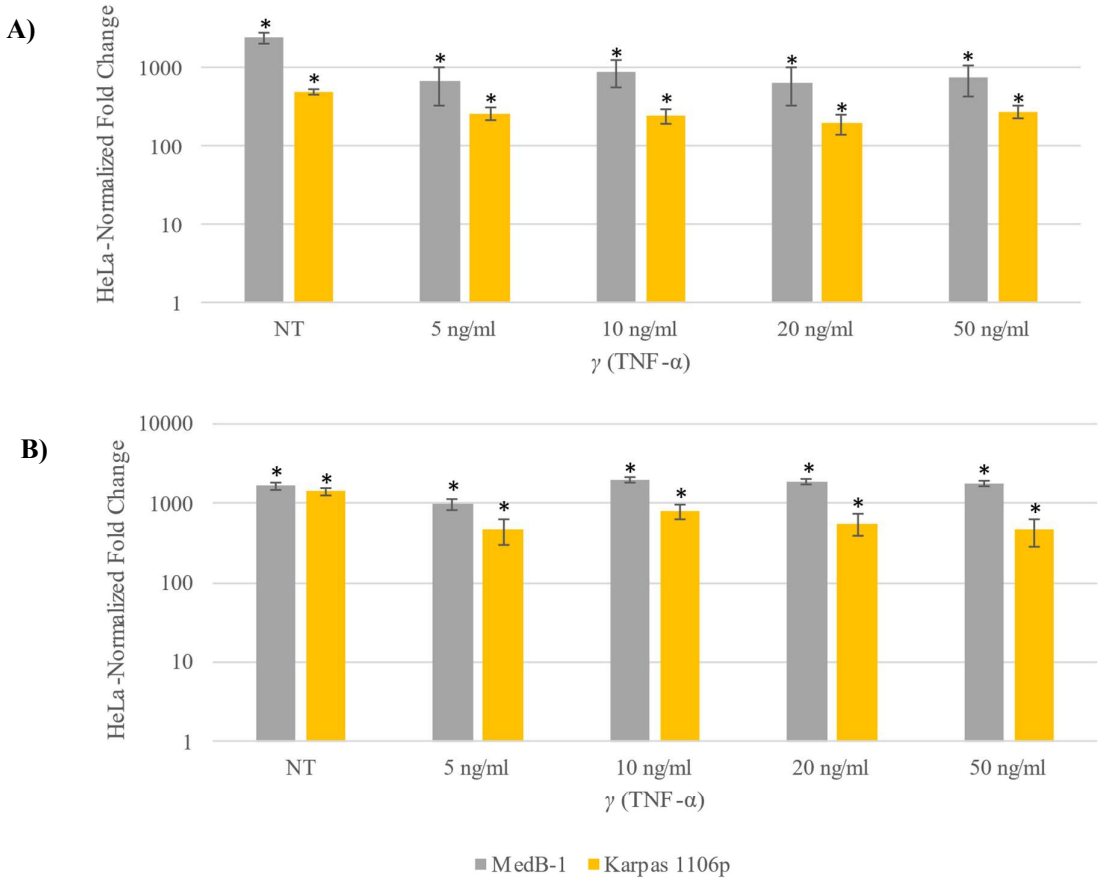

Figure 8. HeLa-normalized fold change in *PDL1* expression in lymphoid cell lines MedB-1 (grey) and Karpas 1106p (yellow) **A)** 24 hours and **B)** 48 hours post-treatment with increasing concentrations of TNF-α. Asterisk (*) marks the statistically significant results determined by independent variable t-test ($p < 0,05$).

4.5. Comparison of gene expression between the lymphoid and epithelial cell lines following IFN-γ treatment

4.5.1. Comparison of *CXCL10* expression between the lymphoid and epithelial cell lines following IFN-γ treatment

At 24 hours post-IFN-γ treatment, both cell lines exhibit an increase in *CXCL10* expression compared to their respective baselines (Figure 9.A). The HFC for MedB-1 increases from 1295 at baseline to 9005 and 9259 at 30 ng/ml and 50 ng/ml doses, respectively. Karpas 1106p cells also show an increase but to a lesser extent, with HFCs of 78 and 47 at the same IFN-γ concentrations.

After 48 hours, the trend in *CXCL10* expression continues to increase for the MedB-1 cell line, with HFCs reaching 275177 at 30 ng/ml and 141130 at 50 ng/ml (Figure 9.B). Karpas 1106p cells, display HFCs of 2228 and 1497 at 30 and 50 ng/ml, respectively. While these numbers represent a significant increase from the 24-hour mark, they are much lower than those observed in MedB-1 cells.

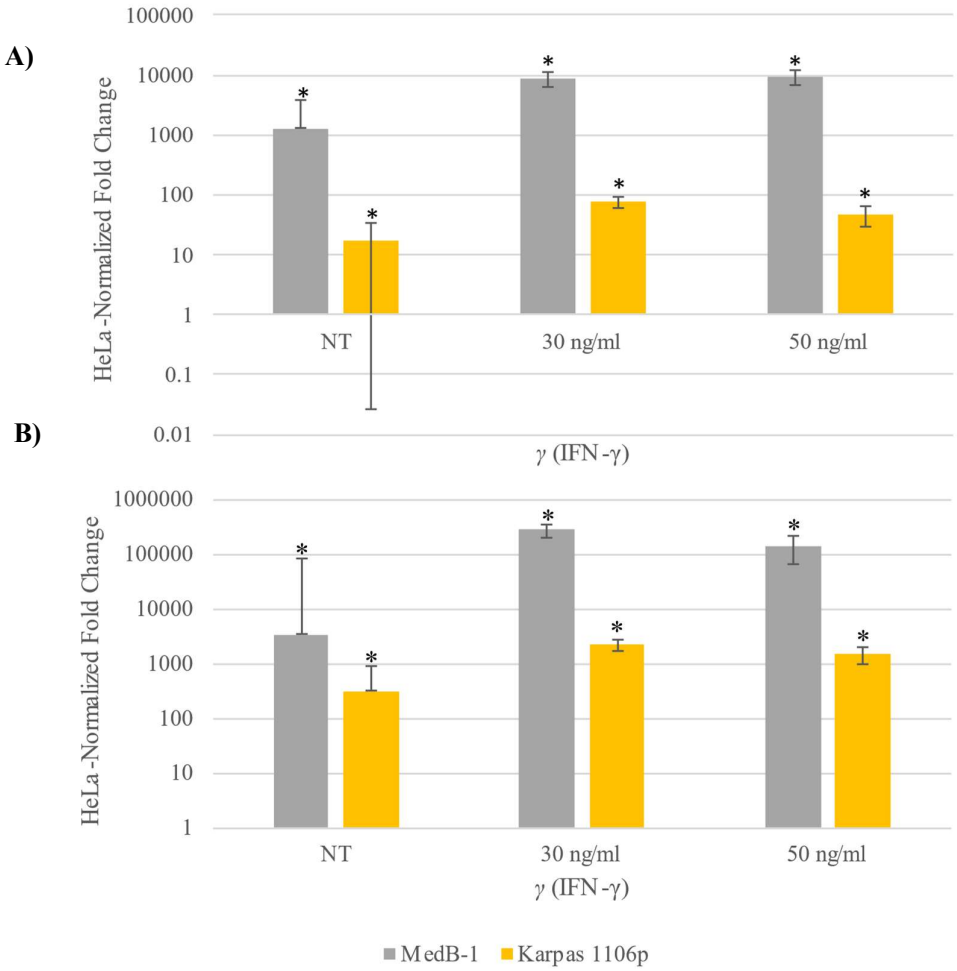

Figure 9. HeLa-normalized fold change in *CXCL10* expression in lymphoid cell lines MedB-1 (grey) and Karpas 1106p (yellow) **A)** 24 hours and **B)** 48 hours post-treatment with increasing concentrations of IFN-γ. Asterisk (*) marks the statistically significant results determined by independent variable t-test ($p < 0,05$).

4.5.2. Comparison of *PDL1* expression between the lymphoid and epithelial cell lines following IFN-γ treatment

Analyzing the HeLa-Normalized Fold Change (HFC) for *PDL1* expression after IFN-γ treatment reveals distinct patterns in MedB-1 and Karpas 1106p cell lines at 24 and 48 hours. At 24 hours post-treatment, MedB-1 cells start with a baseline HFC for *PDL1* of 2391 and exhibit a decrease in expression with increasing concentrations of IFN-γ, reaching an HFC of 432 at 50 ng/ml (Figure 10.A). In Karpas 1106p cells, the baseline HFC is much lower (491), and a similar decreasing trend is observed, with the expression dropping to an HFC of 42 at the highest IFN-γ concentration.

After 48 hours, the HFC in MedB-1 cells decreases from the untreated baseline but shows less reduction at higher IFN-γ concentrations compared to the 24-hour mark, suggesting a stabilizing or adaptive response over time (Figure 10.B). The HFC at 30 ng/ml is 830, which then decreases to 413 at 50 ng/ml. Karpas 1106p cells follow a similar pattern; the HFC decreases from 1394 in untreated cells to 176 at 30 ng/ml and then to 114 at 50 ng/ml IFN-γ.

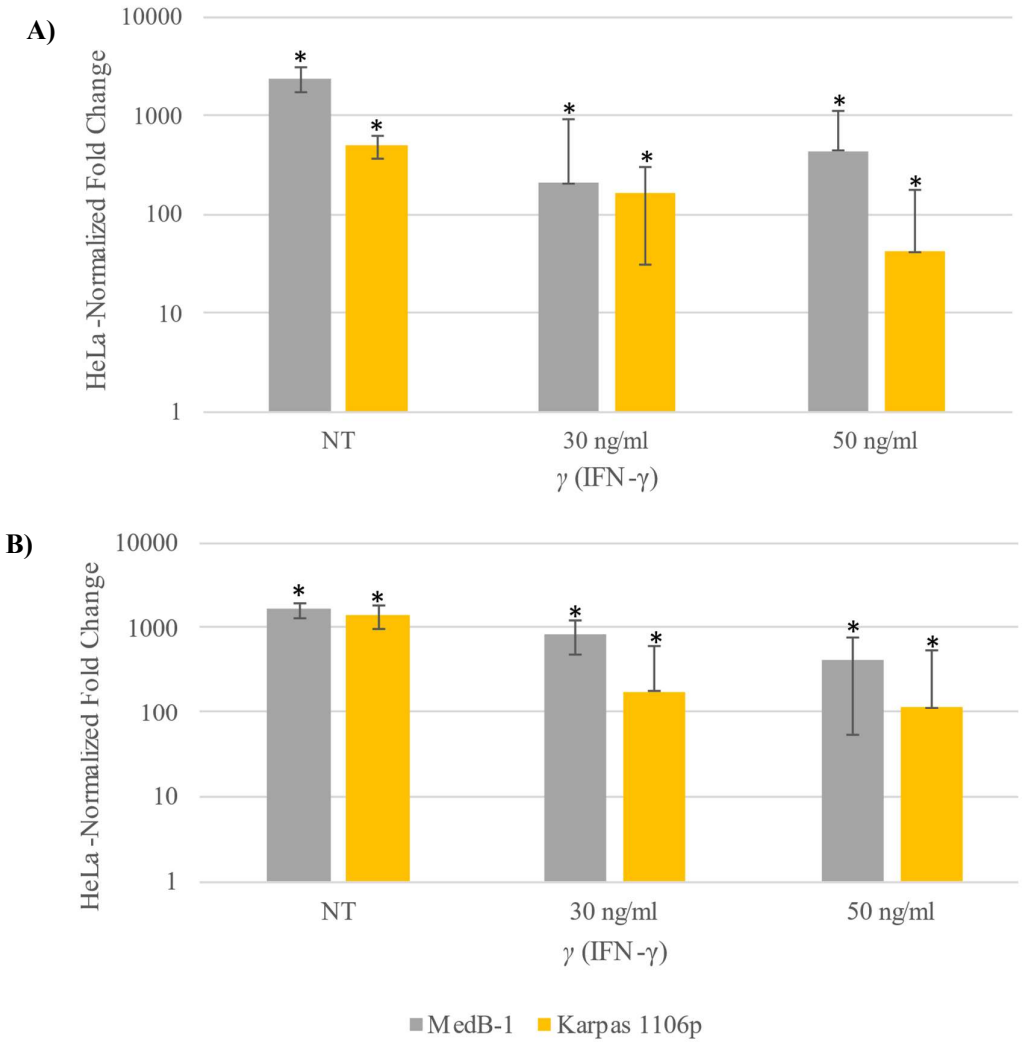

Figure 10. HeLa-normalized fold change in *PDL1* expression in lymphoid cell lines MedB-1 (grey) and Karpas 1106p (yellow) **A)** 24 hours and **B)** 48 hours post-treatment with increasing concentrations of IFN-γ. Asterisk (*) marks the statistically significant results determined by independent variable t-test ($p < 0,05$).

5. Discussion

5.1. *REL* expression

In this study, cell line MedB-1 showed lower *REL* expression after TNF-α tretament during 24 h with all tested concentrations. This suggests that TNF-α might initially trigger pathways to reduce cREL levels, balancing cellular stress or apoptosis signals. In contrast, after 48 hours, *REL* expression had greatly increased, indicating a delayed adaptive response.

Karpas 1106p cells displayed a much more stable and muted response to TNF-α. There were no changes in *REL* expression at any concentration or time point, indicating a relatively consistent *REL* expression profile that appears less sensitive to TNF-α. The stability observed may be attributed to innate differences in the biological processes regulating NF-κB signaling in these cells. Feuerhake et al. (2005) had showed that constitutive activity of this signaling pathway is essential for Karpas 1106 cell survival. It is therefore possible that Karpas 1106p cells have developed mechanisms to protect themselves against variations in TNF-α, keeping the expression of *REL* within a certain range to guarantee the stability and longevity of the cells.

Similarly, HeLa cells showed a relatively stable pattern of *REL* expression in response to TNF-α, with only minor fluctuations. At 24 hours, there was no change in *REL* expression at any concentration. By 48 hours, there was only one statistically significant increase at the lowest concentration, suggesting a minimal sensitivity to TNF-α. The general stability and resistance to large fluctuations suggest that HeLa cells may have a regulatory mechanism that keeps *REL* expression levels constant, independent of the dosage of TNF-α.

Varying *REL* expression patterns in response to TNF-α treatment among cell lines might have important implications for cancer treatments (Kober-Hasslacher & Schmidt-Supprian, 2019). Since cREL regulates genes involved in cell growth and survival, understanding how its expression changes with cytokine signaling might reveal how tumors avoid immune detection and resist cell death (Steidl & Gascoyne, 2011). This evidence suggests the potential to specifically target the NF-κB pathway in distinct types of cancer based on their unique response patterns. This might lead to improved treatment outcomes and fewer side effects. It is important to examine the larger context of NF-κB signaling in immune modulation and cancer formation when analyzing these findings. The relationship between TNF-α and cREL involves typical NF-κB activation pathways and non-canonical pathways, as well as communication with other cellular signaling networks (Steidl & Gascoyne, 2011). The findings of this study reveal that the involvement of the NF-κB signaling cascade in cancer is more complex due to the observed

dose- and time-dependent dynamics. Further research into the molecular processes governing cREL and NF-κB signaling during TNF-α therapy is necessary to identify potential therapeutic targets as well as strategies for cancer treatment.

5.2. *CXCL10* and *PDL1* expression following TNF-α treatment

Among the cell lines studied, only HeLa cells showed a statistically significant increase in *CXCL10* expression following TNF-α treatment. At 24 hours, HeLa cells exhibited an increase in *CXCL10* expression at 5, 10, and 20 ng/ml of TNF-α, indicating a strong and immediate positive response. These results are consistent with previous research by Hardaker et al. (2004), who found that *CXCL10* expression can be induced through NF-κB signaling pathway by TNF-α. MedB-1 cells showed no change in *CXCL10* expression at all TNF-α concentrations at 24 or 48 hours. Likewise, Karpas 1106p cells exhibited no changes in *CXCL10* expression across all concentrations and time points, indicating a stable response to TNF-α. This stability, along with unchanged *CXCL10* exoression, implies that Karpas 1106p cells have mechanisms to tightly regulate *CXCL10* expression, keeping its levels balanced to avoid excessive inflammation.

TNF-α exposure to MedB-1 cells displayed no statistically significant changes in *PDL1* expression 24 hours post-treatment. However, after 48 hours, the cells displayed a dose-dependent increase in *PDL1* expression from 10 to 50 ng/ml. Karpas 1106p cells showed a significant reduction in *PDL1* expression at a 20 ng/ml dose of TNF- α. At 48 hours, the cells showed consistent results, with no changes in *PDL1* expression. A significant increase in *PDL1* expression in HeLa cells 24 hours post-treatment was observed at 5 and 50 ng/ml of TNF-α. By 48 hours, no significant changes in *PDL1* expression were observed. Different studies have already demonstrated TNF-α's ability to upregulate *PDL1* in some malignant tumors (Li et al., 2020; Wang et al., 2017; Hartley et al., 2017). Additionally, some studies have shown that targeting key signaling pathways can have significant therapeutic effects. For example, amorfrutin A has been shown to block JAK/STAT3 signaling and STAT3 activity in HeLa cells, thereby downregulating genes linked to cell survival and proliferation as well as displaying anti-tumor effects in a HeLa xenograft model (Mi et al., 2017). This implies that similar targeted approaches could be investigated for the purpose of modulating *PDL1* and other immune checkpoints in therapy for different malignant tumors.

5.3. Impact of IFN-γ on gene expression

In MedB-1 cells 24 hours post-treatment, *CXCL10* expression had increased 264-fold at 30 ng/ml and 525-fold at 50 ng/ml. Expression of *CXCL10* in Karpas 1106p cells increased 169-

fold at 30 ng/ml and 199-fold at 50 ng/ml. HeLa cells did not show statistically significant changes in *CXCL10* expression. This substantial increase suggests a pronounced responsiveness of lymphoma cells to IFN-γ. At 48 hours, all cell lines show significant increase in *CXCL10* expression. In MedB-1 cells, it had increased 1245-fold at 30 ng/ml and 1072-fold at 50 ng/ml. Karpas 1106p cells showed 109-fold increase in expression at 30 ng/ml and 123-fold at 50 ng/ml. In HeLa cells, *CXCL10* expression increased 15-fold at 30 ng/ml and 26-fold at 50 ng/ml. *CXCL10* upregulation in Karpas 1106p cells, although less than that in MedB-1, along with the significant yet lesser changes in HeLa cells, shows the variability in IFN-γ signaling pathways among different cell lines and different tumor types. Gene expression patterns after IFN-γ therapy indicate significant JAK/STAT pathway activation, promoting antiviral defenses and anti-proliferative effects in tumors. This is consistent with previous reports where CXCL10 was shown to attract CXCR3+ CD8+ T cells and induce their cytotoxic activity via granzyme B production, thereby enhancing anti-tumor responses (Barreira da Silva et al., 2015; Lees et al., 2019). Particularly after 48 hours, the *CXCL10* increase points to continuous activation and might therefore improve the effectiveness of immune checkpoint blocking treatments.

Similarly, the upregulation of *PDL1* in response to IFN-γ treatment across the studied cell lines brings attention to the delicate balance that must be achieved in anti-tumor immunity. 24 hours after IFN-γ treatment, *PDL1* expression in MedB-1 cells did not change. Karpas 1106p cells exhibited slight but statistically significant increases, with a 1.6-fold rise at 30 ng/ml and a 1.8-fold increase at 50 ng/ml. HeLa cells showed significant changes with a 17-fold increase at 30 ng/ml and a 21-fold increase at 50 ng/ml. 48 hours post-treatment, *PDL1* expression in MedB-1 cells had a significant 8-fold increase at 30 ng/ml and 5-fold at 50 ng/ml. Karpas 1106p cells exhibited a 2-fold increase at 30 ng/ml, and HeLa cells maintained almost exactly the same *PDL1* expression levels recorded at a 24-hour time point at both concentrations. While the increase of *PDL1* may appear contradictory in an anti-tumor setting, considering its participation in immune checkpoint pathways, it is critical to consider this within the context of the cancer-immunity cycle. Elevated production of *PDL1* in response to IFN-γ has been demonstrated in various cancer types, including pancreatic, gastric, and colorectal cancer, as well as myeloid leukemia (Imai et al., 2019; Mimura et al., 2018; Zhao et al., 2020; Bellucci et al., 2015). However, the enhanced *PDL1* expression also offers a possible target for checkpoint inhibitor treatments, like nivolumab and brentuximab vedotin, which showed long-term efficacy in CheckMate 436 study (Katsuya et al., 2023; Zinzani et al., 2019; Zinzani et al., 2023). This illustrates the dual function of IFN-γ: it may both boost anti-tumor immunity and

enable immune escape, therefore stressing the complexity of the role it plays in the immune response to cancer.

5.4. Comparison between cell lines

HFC values for all genes in all treatment conditions were positive, meaning that baseline expression levels of *REL*, *PDL1* and *CXCL10* are higher in PMBCL-derived cell lines than in epithelial cell line HeLa, which was expected given PMBCL's dependence on constitutive activity of NF-κB and JAK-STAT pathways (Steidl & Gascoyne, 2011). The somewhat similar baseline expression levels of MedB-1 and Karpas 1106p cells for *REL* point to a basic role for cREL in preserving basic cellular activities linked to growth and survival in both lymphoma cell lines. Greater *REL* expression in MedB-1, however, may be a marker of a stronger dependence on NF-κB signaling, which may help to explain the more aggressive character of PMBCL relative to other lymphoma subtypes.

Known for its function in immune checkpoint pathways, the *PDL1* gene shows quite distinct baseline expression in MedB-1 and Karpas 1106p cell lines. Normalizing the FC values versus HeLa cells reveals that MedB-1 cells express *PDL1* at about 2000 times the baseline level, while Karpas 1106p cells show HFCs in a range of 500 to 1500. Natural genetic or epigenetic variations across these cell lines could explain this disparity and might affect the stability of PDL1 mRNA or the transcriptional machinery.

When comparing *CXCL10* expression, MedB-1 and Karpas 1106p cells show more noticeable differences. MedB-1 cells have an HFC of 1300 to 3300, far greater than that of Karpas 1106p cells, which was from 17 to 315. The higher baseline levels in MedB-1 cells point to a more inflammatory condition, which might help to recruit immune cells that could promote tumor development and survival by means of either an immunosuppressive environment or angiogenesis. There are many elements which might explain the variations in baseline gene expression among these cell lines. Likely factors include genetic variances including variations in gene amplification or chromosomal changes. For example, the amplification of genes like *REL* and *PDL1* in PMBCL might naturally raise their expression as shown in MedB-1 cells. Epigenetic changes like histone modifications and methylation state can also influence gene expression without changing the DNA sequence. Moreover, variations in the TME – including those in cytokine and chemokine levels – may affect gene expression via paracrine or autocrine signaling pathways (Yi et al, 2021).

5.5. Limitations and considerations

While this study offers valuable insights into how TNF-α and IFN-γ influence gene expression in cancer cell lines, there are several important limitations to consider. Primarily, my research was carried out *in vitro*, which, although providing valuable insights, cannot completely mimic the intricate and varied conditions seen in the TME within a living organism. The interactions occurring within the TME, which involve the presence of different immune cells, extracellular matrix components, and other stromal factors, have a substantial impact on the behavior of cancer cells and their reaction to cytokines (Dranoff, 2004). Another important factor to consider is the utilization of cell lines as models. Cell lines, while valuable for researching malignant cell biology, may not completely represent the genetic and epigenetic diversity observed in actual patient malignancies (Dai et al., 2015). Cancers display substantial variability, which has a profound impact on treatment outcomes. To address this discrepancy, future investigations should incorporate *in vivo* experiments utilizing animal models or clinical trials to verify these findings and assess the therapeutic efficacy and safety of targeting these cytokine pathways in a more practical environment. Moreover, our focus was limited to TNF-α and IFN-γ, but the cytokine network in the TME is far more complex (Munn & Bronte, 2016; Yi et al., 2021). A multitude of cytokines, growth factors, and signaling molecules engage in a complex and interconnected network of interactions. Examining the interaction among TNF-α, IFN-γ, and other cytokines may uncover synergistic or antagonistic relationships that could be utilized for improving treatment methods, as some studies have already shown (Hardaker et al., 2004; English et al., 2007). By doing a more extensive investigation, we could obtain a more thorough knowledge of the regulatory networks that control tumor biology.

6. Conclusion

- Baseline expression of *REL*, *CXCL10,* and *PDL1* is higher in PMBCL-derived cell lines than in human cervical carcinoma-derived cell line HeLa.
- 48 hours after TNF-α treatment, *REL* and *PDL1* expression had significantly increased in MedB-1 cells in a dose-dependent manner at 10, 20, and 50 ng/ml.
- HeLa cells showed statistically significant increase in *CXCL10* expression 24 hours after treatment with 5, 10, and 20 ng/ml TNF-α.
- MedB-1 and Karpas 1106p cells showed no statistically significant changes in *CXCL10* expression after tretament with TNF-α.
- IFN-γ treatment increased *CXCL10* expression in all cell lines studied.
- After IFN-γ treatment, *PDL1* expression increased in all cell lines studied, with HeLa cells showing more pronounced and stable response than PMBCL-derived cell lines.

7. References

1. Akdis, M., Aab, A., Altunbulakli, C., Azkur, K., Costa, R. A., Crameri, R., ... & Akdis, C. A. (2016). Interleukins (from IL-1 to IL-38), interferons, transforming growth factor β, and TNF-α: Receptors, functions, and roles in diseases. *Journal of Allergy and Clinical Immunology*, *138*(4), 984-1010.
2. Arenberg, D. A., White, E. S., Burdick, M. D., Strom, S. R., & Strieter, R. M. (2001). Improved survival in tumor-bearing SCID mice treated with interferon-γ-inducible protein 10 (IP-10/CXCL10). *Cancer Immunology, Immunotherapy*, *50*, 533-538.
3. Bach, E. A., Aguet, M., & Schreiber, R. D. (1997). The IFNγ receptor: a paradigm for cytokine receptor signaling. *Annual Review of Immunology*, *15*(1), 563-591.
4. Balkwill, F. (2009). Tumour necrosis factor and cancer. *Nature Reviews Cancer*, *9*(5), 361-371.
5. Barreira da Silva, R., Laird, M. E., Yatim, N., Fiette, L., Ingersoll, M. A., & Albert, M. L. (2015). Dipeptidylpeptidase 4 inhibition enhances lymphocyte trafficking, improving both naturally occurring tumor immunity and immunotherapy. *Nature Immunology*, 16(8), 850-858.
6. Bea, S., Zettl, A., Wright, G., Salaverria, I., Jehn, P., Moreno, V., ... & Lymphoma/Leukemia Molecular Profiling Project. (2005). Diffuse large B-cell lymphoma subgroups have distinct genetic profiles that influence tumor biology and improve gene-expression-based survival prediction. *Blood*, *106*(9), 3183-3190.
7. Bellucci, R., Martin, A., Bommarito, D., Wang, K., Hansen, S. H., Freeman, G. J., & Ritz, J. (2015). Interferon-γ-induced activation of JAK1 and JAK2 suppresses tumor cell susceptibility to NK cells through upregulation of PD-L1 expression. *OncoImmunology*, *4*(6).
8. Bentz, M., Barth, T. F., Brüderlein, S., Bock, D., Schwerer, M. J., Baudis, M., ... & Möller, P. (2001). Gain of chromosome arm 9p is characteristic of primary mediastinal B-cell lymphoma (MBL): comprehensive molecular cytogenetic analysis and presentation of a novel MBL cell line. *Genes, Chromosomes and Cancer*, *30*(4), 393-401.
9. Boehm, U., Klamp, T., Groot, M., & Howard, J. C. (1997). Cellular responses to interferon-γ. *Annual Review of Immunology*, *15*(1), 749-795.
10. Bradley, J. (2008). TNF-mediated inflammatory disease. *The Journal of Pathology: A Journal of the Pathological Society of Great Britain and Ireland*, *214*(2), 149-160.

11. Campo, E., Swerdlow, S. H., Harris, N. L., Pileri, S., Stein, H., & Jaffe, E. S. (2011). The 2008 WHO classification of lymphoid neoplasms and beyond: evolving concepts and practical applications. *Blood, The Journal of the American Society of Hematology*, *117*(19), 5019-5032.
12. Cancer Genome Atlas Research Network. (2017). Integrated genomic and molecular characterization of cervical cancer. *Nature*, *543*(7645), 378.
13. Chen T. R. (1988). Re-evaluation of HeLa, HeLa S3, and HEp-2 karyotypes. *Cytogenetics and Cell Genetics*, *48*(1), 19–24.
14. Dai, H., Ehrentraut, S., Nagel, S., Eberth, S., Pommerenke, C., Dirks, W. G., Geffers, R., Kalavalapalli, S., Kaufmann, M., Meyer, C., Faehnrich, S., Chen, S., Drexler, H. G., & MacLeod, R. A. (2015). Genomic Landscape of Primary Mediastinal B-Cell Lymphoma Cell Lines. *PloS one*, *10*(11),
15. Darnell Jr, J. E., Kerr, L. M., & Stark, G. R. (1994). Jak-STAT pathways and transcriptional activation in response to IFNs and other extracellular signaling proteins. *Science*, *264*(5164), 1415-1421.
16. Dinarello, C. A. (2007). Historical insights into cytokines. *European Journal of Immunology*, *37*(S1), S34-S45.
17. Dranoff, G. (2004). Cytokines in cancer pathogenesis and cancer therapy. *Nature Reviews Cancer*, *4*(1), 11-22.
18. English, K., Barry, F. P., Field-Corbett, C. P., & Mahon, B. P. (2007). IFN-γ and TNF-α differentially regulate immunomodulation by murine mesenchymal stem cells. *Immunology Letters*, *110*(2), 91-100.
19. Feuerhake, F., Kutok, J. L., Monti, S., Chen, W., LaCasce, A. S., Cattoretti, G., ... & Shipp, M. A. (2005). NFκB activity, function, and target-gene signatures in primary mediastinal large B-cell lymphoma and diffuse large B-cell lymphoma subtypes. *Blood*, *106*(4), 1392-1399.
20. Gey, G. (1952). Tissue culture studies of the proliferative capacity of cervical carcinoma and normal epithelium. *Cancer Research*, *12*, 264-265.
21. Hao, Y., Chapuy, B., Monti, S., Sun, H. H., Rodig, S. J., & Shipp, M. A. (2014). Selective JAK2 inhibition specifically decreases Hodgkin lymphoma and mediastinal large B-cell lymphoma growth in vitro and in vivo. *Clinical Cancer Research*, *20*(10), 2674-2683.
22. Hardaker, E. L., Bacon, A. M., Carlson, K., Roshak, A. K., Foley, J. J., Schmidt, D. B., ... & Belmonte, K. E. (2004). Regulation of TNF-α and IFN-γ induced CXCL10 expression: participation of the airway smooth muscle in the pulmonary inflammatory

response in chronic obstructive pulmonary disease. *The FASEB Journal*, *18*(1), 191-193.

23. Hartley, G., Regan, D., Guth, A., & Dow, S. (2017). Regulation of PD-L1 expression on murine tumor-associated monocytes and macrophages by locally produced TNF-α. *Cancer Immunology, Immunotherapy*, *66*, 523-535.
24. Imai, D., Yoshizumi, T., Okano, S., Itoh, S., Ikegami, T., Harada, N., Aishima, S., Oda, Y., & Maehara, Y. (2019). IFN-γ promotes epithelial-mesenchymal transition and the expression of PD-L1 in pancreatic cancer. *Journal of Surgical Research, 240*, 115-123.
25. Joos, S., Otaño-Joos, M. I., Ziegler, S., Bruderlein, S., Du Manoir, S., Bentz, M., ... & Lichter, P. (1996). Primary mediastinal (thymic) B-cell lymphoma is characterized by gains of chromosomal material including 9p and amplification of the REL gene. *Blood, 87*(4), 1571-1578.
26. Kaplan, D. H., Shankaran, V., Dighe, A. S., Stockert, E., Aguet, M., Old, L. J., & Schreiber, R. D. (1998). Demonstration of an interferon γ-dependent tumor surveillance system in immunocompetent mice. *Proceedings of the National Academy of Sciences*, *95*(13), 7556-7561.
27. Kaplan, G. I. L. L. A., Luster, A. D., Hancock, G. E. R. A. L. D., & Cohn, Z. (1987). The expression of a gamma interferon-induced protein (IP-10) in delayed immune responses in human skin. *The Journal of Experimental Medicine*, *166*(4), 1098-1108.
28. Karin, N., & Razon, H. (2018). Chemokines beyond chemo-attraction: CXCL10 and its significant role in cancer and autoimmunity. *Cytokine*, *109*, 24-28.
29. Katsuya, H., Suzumiya, J., & Kimura, S. (2023). Clinical PD-1/PD-L1 Blockades in Combination Therapies for Lymphomas. *Cancers*, *15*(22), 5399.
30. Kinjyo, I., Hanada, T., Inagaki-Ohara, K., Mori, H., Aki, D., Ohishi, M., ... & Yoshimura, A. (2002). SOCS1/JAB is a negative regulator of LPS-induced macrophage activation. *Immunity*, *17*(5), 583-591.
31. Kishimoto, T. (2005). Interleukin-6: from basic science to medicine—40 years in immunology. *Annual Review of Immunology*, *23*, 1-21.
32. Kober-Hasslacher, M., & Schmidt-Supprian, M. (2019). The unsolved puzzle of c-Rel in B cell lymphoma. *Cancers*, *11*(7), 941.
33. Kumar, A., Commane, M., Flickinger, T. W., Horvath, C. M., & Stark, G. R. (1997). Defective TNF-α-induced apoptosis in STAT1-null cells due to low constitutive levels of caspases. *Science*, *278*(5343), 1630-1632.

34. Landry, J. J., Pyl, P. T., Rausch, T., Zichner, T., Tekkedil, M. M., Stütz, A. M., ... & Steinmetz, L. M. (2013). The genomic and transcriptomic landscape of a HeLa cell line. *G3: Genes, Genomes, Genetics*, *3*(8), 1213-1224.
35. Lee, S., Shah, T., Yin, C., Hochberg, J., Ayello, J., Morris, E., ... & Cairo, M. S. (2018). Ruxolitinib significantly enhances in vitro apoptosis in Hodgkin lymphoma and primary mediastinal B-cell lymphoma and survival in a lymphoma xenograft murine model. *Oncotarget*, *9*(11), 9776.
36. Lees, C., Keane, C., Gandhi, M. K., & Gunawardana, J. (2019). Biology and therapy of primary mediastinal B-cell lymphoma: current status and future directions. *British Journal of Haematology*, *185*(1), 25-41.
37. Lenz, G., Wright, G. W., Emre, N. T., Kohlhammer, H., Dave, S. S., Davis, R. E., ... & Staudt, L. M. (2008). Molecular subtypes of diffuse large B-cell lymphoma arise by distinct genetic pathways. *Proceedings of the National Academy of Sciences*, *105*(36), 13520-13525.
38. Li, Z., Zhang, C., Du, J. X., Zhao, J., Shi, M. T., Jin, M. W., & Liu, H. (2020). Adipocytes promote tumor progression and induce PD-L1 expression via TNF-α/IL-6 signaling. *Cancer Cell International*, *20*, 1-9.
39. Lienard, D., Ewalenko, P., Delmotte, J. J., Renard, N., & Lejeune, F. J. (1992). High-dose recombinant tumor necrosis factor alpha in combination with interferon gamma and melphalan in isolation perfusion of the limbs for melanoma and sarcoma. *Journal of Clinical Oncology*, *10*(1), 52-60.
40. Livak, K. J., & Schmittgen, T. D. (2001). Analysis of relative gene expression data using real-time quantitative PCR and the 2− ΔΔCT method. *Methods*, *25*(4), 402-408.
41. Luster, A. D., & Ravetch, J. V. (1987). Biochemical characterization of a gamma interferon-inducible cytokine (IP-10). *The Journal of Experimental Medicine*, *166*(4), 1084-1097.
42. Martelli, M., Ferreri, A., Di Rocco, A., Ansuinelli, M., & Johnson, P. W. (2017). Primary mediastinal large B-cell lymphoma. *Critical Reviews in Oncology/Hematology*, *113*, 318-327.
43. Masters, J. R. (2002). HeLa cells 50 years on: the good, the bad and the ugly. *Nature Reviews Cancer*, *2*(4), 315-319.
44. Meissner, J. D. (1999). Nucleotide sequences and further characterization of human papillomavirus DNA present in the CaSki, SiHa and HeLa cervical carcinoma cell lines. *Journal of General Virology*, *80*(7), 1725-1733.

45. Mi, C., Ma, J., Wang, K. S., Wang, Z., Li, M. Y., Li, J. B., ... & Jin, X. (2017). Amorfrutin A inhibits TNF-α induced JAK/STAT signaling, cell survival and proliferation of human cancer cells. *Immunopharmacology and Immunotoxicology*, *39*(6), 338-347.
46. Mimura, K., Teh, J. L., Okayama, H., Shiraishi, K., Kua, L. F., Koh, V., Smoot, D. T., Ashktorab, H., Oike, T., Suzuki, Y., & et al. (2018). PD-L1 expression is mainly regulated by interferon gamma associated with JAK-STAT pathway in gastric cancer. *Cancer Science, 109*(1), 43-53.
47. Miscia, S., Marchisio, M., Grilli, A., Di Valerio, V., Centurione, L., Sabatino, G., ... & Di Baldassarre, A. (2002). Tumor necrosis factor α (TNF-α) activates Jak1/Stat3-Stat5B signaling through TNFR-1 in human B cells. *Cell Growth & Differentiation*, *13*(1), 13-18.
48. Möller, P., Brüderlein, S., Sträter, J., Leithäuser, F., Hasel, C., Bataille, F., Moldenhauer, G., Pawlita, M., & Barth, T. F. (2001). MedB-1, a human tumor cell line derived from a primary mediastinal large B-cell lymphoma. *International Journal of Cancer*, *92*(3), 348-353.
49. Moore, K. W., de Waal Malefyt, R., Coffman, R. L., & O'Garra, A. (2001). Interleukin-10 and the interleukin-10 receptor. *Annual Review of Immunology, 19*(1), 683-765.
50. Munn, D. H., & Bronte, V. (2016). Immune suppressive mechanisms in the tumor microenvironment. *Current Opinion in Immunology*, *39*, 1-6.
51. Nacheva, E., Dyer, M. J., Metivier, C., Jadayel, D., Stranks, G., Morilla, R., Heward, J. M., Holloway, T., O'Connor, S., & Bevan, P. C. (1994). B-cell non-Hodgkin's lymphoma cell line (Karpas 1106) with complex translocation involving 18q21.3 but lacking BCL2 rearrangement and expression. *Blood*, 84(10), 3422-3428.
52. Nakagawa, R., Naka, T., Tsutsui, H., Fujimoto, M., Kimura, A., Abe, T., ... & Kishimoto, T. (2002). SOCS-1 participates in negative regulation of LPS responses. *Immunity*, *17*(5), 677-687.
53. Nicholas, N. S., Apollonio, B., & Ramsay, A. G. (2016). Tumor microenvironment (TME)-driven immune suppression in B cell malignancy. *Biochimica et Biophysica Acta (BBA)-Molecular Cell Research*, *1863*(3), 471-482.
54. O'Shea, J. J., Ma, A., & Lipsky, P. (2002). Cytokines and autoimmunity. *Nature Reviews Immunology*, *2*(1), 37-45.
55. Pater, M. M., & Pater, A. (1985). Human papillomavirus types 16 and 18 sequences in carcinoma cell lines of the cervix. *Virology*, *145*(2), 313–318.

56. Roberts, R. A., Wright, G., Rosenwald, A. R., Jaramillo, M. A., Grogan, T. M., Miller, T. P., ... & Rimsza, L. M. (2006). Loss of major histocompatibility class II gene and protein expression in primary mediastinal large B-cell lymphoma is highly coordinated and related to poor patient survival. *Blood*, *108*(1), 311-318.
57. Schiffman, M., Wentzensen, N., Wacholder, S., Kinney, W., Gage, J. C., & Castle, P. E. (2011). Human papillomavirus testing in the prevention of cervical cancer. *Journal of the National Cancer Institute*, *103*(5), 368-383.
58. Schmidt, M. W., Battista, M. J., Schmidt, M., Garcia, M., Siepmann, T., Hasenburg, A., & Anic, K. (2022). Efficacy and safety of immunotherapy for cervical cancer—A systematic review of clinical trials. *Cancers*, *14*(2), 441.
59. Schroder, K., Hertzog, P. J., Ravasi, T., & Hume, D. A. (2004). Interferon-γ: an overview of signals, mechanisms and functions. *Journal of Leucocyte Biology*, *75*(2), 163-189.
60. Shen, C. H. (2019). Detection and analysis of nucleic acids. *Diagnostic Molecular Biology*, 167-185.
61. Shi, M., Roemer, M. G., Chapuy, B., Liao, X., Sun, H., Pinkus, G. S., ... & Rodig, S. J. (2014). Expression of programmed cell death 1 ligand 2 (PD-L2) is a distinguishing feature of primary mediastinal (thymic) large B-cell lymphoma and associated with PDCD1LG2 copy gain. *The American Journal of Surgical Pathology*, *38*(12), 1715-1723.
62. Shuai, K., & Liu, B. (2003). Regulation of JAK–STAT signalling in the immune system. *Nature Reviews Immunology*, *3*(11), 900-911.
63. Steidl, C., & Gascoyne, R. D. (2011). The molecular pathogenesis of primary mediastinal large B-cell lymphoma. *Blood, The Journal of the American Society of Hematology*, *118*(10), 2659-2669.
64. Steidl, C., Shah, S. P., Woolcock, B. W., Rui, L., Kawahara, M., Farinha, P., ... & Gascoyne, R. D. (2011). MHC class II transactivator CIITA is a recurrent gene fusion partner in lymphoid cancers. *Nature*, *471*(7338), 377-381.
65. Tanaka, T., Nishie, R., Ueda, S., Miyamoto, S., Hashida, S., Konishi, H., ... & Ohmichi, M. (2021). Patient-derived xenograft models in cervical cancer: a systematic review. *International Journal of Molecular Sciences*, *22*(17), 9369.
66. Tracey, D., Klareskog, L., Sasso, E. H., Salfeld, J. G., & Tak, P. P. (2008). Tumor necrosis factor antagonist mechanisms of action: a comprehensive review. *Pharmacology & Therapeutics*, *117*(2), 244-279.

67. Twa, D. D., Chan, F. C., Ben-Neriah, S., Woolcock, B. W., Mottok, A., Tan, K. L., ... & Steidl, C. (2014). Genomic rearrangements involving programmed death ligands are recurrent in primary mediastinal large B-cell lymphoma. *Blood, The Journal of the American Society of Hematology*, *123*(13), 2062-2065.
68. Vallabhapurapu, S., & Karin, M. (2009). Regulation and function of NF-κB transcription factors in the immune system. *Annual Review of Immunology*, *27*, 693-733.
69. Walboomers, J. M., Jacobs, M. V., Manos, M. M., Bosch, F. X., Kummer, J. A., Shah, K. V., ... & Muñoz, N. (1999). Human papillomavirus is a necessary cause of invasive cervical cancer worldwide. *The Journal of Pathology*, *189*(1), 12-19.
70. Wang, X., Yang, L., Huang, F., Zhang, Q., Liu, S., Ma, L., & You, Z. (2017). Inflammatory cytokines IL-17 and TNF-α up-regulate PD-L1 expression in human prostate and colon cancer cells. *Immunology Letters*, *184*, 7-14.
71. Weniger, M. A., Gesk, S., Ehrlich, S., Martin-Subero, J. I., Dyer, M. J., Siebert, R., ... & Barth, T. F. (2007). Gains of REL in primary mediastinal B-cell lymphoma coincide with nuclear accumulation of REL protein. *Genes, Chromosomes and Cancer*, *46*(4), 406-415.
72. Xie, M., Huang, X., Ye, X., & Qian, W. (2019). Prognostic and clinicopathological significance of PD-1/PD-L1 expression in the tumor microenvironment and neoplastic cells for lymphoma. *International Immunopharmacology, 105999.*
73. Yi, M., Niu, M., Xu, L., Luo, S., & Wu, K. (2021). Regulation of PD-L1 expression in the tumor microenvironment. *Journal of Hematology & Oncology*, *14*(1), 1-13.
74. Zhao, T., Li, Y., Zhang, J., & Zhang, B. (2020). PD-L1 expression increased by IFN-γ via JAK2-STAT1 signaling and predicts a poor survival in colorectal cancer. *Oncology Letters*, *20*, 1127-1134.
75. Zheng, X., Zhu, Y., Wang, X., Hou, Y., & Fang, Y. (2021). Silencing of ITGB6 inhibits the progression of cervical carcinoma via regulating JAK/STAT3 signaling pathway. *Annals of Translational Medicine*, *9*(9).
76. Zinzani, P. L., Santoro, A., Gritti, G., Brice, P., Barr, P. M., Kuruvilla, J., ... & Moskowitz, A. J. (2019). Nivolumab combined with brentuximab vedotin for relapsed/refractory primary mediastinal large B-cell lymphoma: efficacy and safety from the phase II CheckMate 436 study. *Journal of Clinical Oncology*, *37*(33), 3081.
77. Zinzani, P. L., Santoro, A., Gritti, G., Brice, P., Barr, P. M., Kuruvilla, J., ... & Moskowitz, A. J. (2023). Nivolumab combined with brentuximab vedotin for R/R

primary mediastinal large B-cell lymphoma: a 3-year follow-up. *Blood Advances*, *7*(18), 5272-5280.

CV

My name is Valentino Mihalić. I was born on October 7, 1999 in Karlovac, Croatia. I received my high school education at the Karlovac Gymnasium, and then I completed the undergraduate study of Molecular Biology at the Faculty of Science and Mathematics of the University of Zagreb, where I am currently attending the graduate study of Molecular Biology. As part of the Laboratory practice under the guidance of associate professor Tomislav Ivanković, PhD, at the Institute of Microbiology, I participated in the creation of the scientific paper "Perlite as a Biocarrier for Augmentation of Biogas-Producing Reactors from Olive (*Olea europaea*) Waste" published in 2022 in the journal Applied Sciences (https://doi.org/10.3390/app12178808). During my undergraduate studies, as a member of the Board of Directors of the Biology Students' Association – BIUS and head of the Bats Section, I participated in 3 research and educational projects: Insula Auri 2019, Žumberak 2020 and Žumberak 2021.